

# Abelian and non-Abelian topological behavior of a neutral spin-1/2 particle in a background magnetic field.\*

B. Zygelman

*Department of Physics and Astronomy, University of Nevada, Las Vegas, USA*

We present results of a numerical experiment in which a neutral spin-1/2 particle subjected to a static magnetic vortex field passes through a double-slit barrier. We demonstrate that the resulting interference pattern on a detection screen exhibits fringes reminiscent of Aharonov-Bohm scattering by a magnetic flux tube. To gain better understanding of the observed behavior, we provide analytic solutions for a neutral spin-1/2 rigid planar rotor in the aforementioned magnetic field. We demonstrate how that system exhibits a non-Abelian Aharonov-Bohm effect due to the emergence of an effective Wu-Yang (WY) flux tube. We study the behavior of the gauge invariant partition function and demonstrate a topological phase transition for the spin-1/2 planar rotor. We provide an expression for the partition function in which its dependence on the Wilson loop integral of the WY gauge potential is explicit. We generalize to a spin-1 system in order to explore the Wilczek-Zee (WZ) mechanism in a full quantum setting. We show how degeneracy can be lifted by higher order gauge corrections that alter the semi-classical, non-Abelian, WZ phase. Models that allow analytic description offer a foil to objections that question the fidelity of predictions based on the generalized Born-Oppenheimer approximation in atomic and molecular systems.

Though the primary focus of this study concerns the emergence of gauge structure in neutral systems, the theory is also applicable to systems that possess electric charge. In that case, we explore interference between fundamental gauge fields (i.e. electromagnetism) with effective gauge potentials. We propose a possible laboratory demonstration for the latter in an ion trap setting. We illustrate how effective gauge potentials influence wave-packet revivals in the said ion trap.

## I. INTRODUCTION

The double slit experiment and the Aharonov-Bohm (AB) effect[1] are iconic examples that highlight novel and counter-intuitive aspects of the quantum theory[2]. The former has long served as a pedagogical device[3] to introduce the notion of wave-particle duality to students of quantum mechanics and laboratory demonstrations of it have raised new questions regarding the role of measurement in quantum mechanics (QM) [4, 5]. The AB effect demonstrates the role of gauge potentials in quantum mechanics, and Feynman[3] framed it in a double slit setting to illustrate and underscore its topological significance.

From the Einstein-Bohr-Sommerfeld quantization rules to the TKNN integers[6], topology has always played a role in QM, and for which the AB effect offers an instructive template. It has been applied to elaborate on the nature of anyons[7] and other forms of exotic quantum matter[8]. Researchers hope to harness topology in service of enabling high-fidelity qubit technology[9] and fault tolerant quantum computing[10].

In this paper we illustrate how AB-like topological effects, and its non-Abelian generalization[11, 12], manifest in simple quantum systems that allow accurate numerical as well as analytic solutions. First, we consider the dynamics of a neutral spin-1/2 system coupled to an external static magnetic field. We perform a quantum mechanical numerical experiment in which the particle

passes through a double-slit barrier. When the position of the particle is measured at a detection screen we find an anticipated wave interference pattern.

In addition to interference due to the presence of slit barriers, we show that the resulting pattern is best described by appealing to a model in which a charged particle is minimally coupled to an effective magnetic flux tube. This, despite the fact that the spin-1/2 particle is neutral and couples locally to the external field via the standard  $\vec{\mu} \cdot \vec{B}$  term.

Our numerical experiment provides a demonstration of how effective gauge potentials arise in quantum systems that appear to have no overt gauge structure. This system (without the double slit) was first proposed[13] as an example of inertial frame dragging. Here we confirm, via our numerical simulation, the predictions of that gedanken system. In addition to the predicted[13] Abelian AB behavior, we explore non-Abelian features inherent in analogous systems that allow analytic solution.

In section II, we summarize the results of our numerical experiment. We demonstrate the scattering of a neutral spin-1/2 wave-packet by a double slit barrier. The packet experiences a background magnetic field  $\vec{B}$  in which the condition  $\vec{\nabla}(\vec{\mu} \cdot \vec{B}) = 0$ , is satisfied. The latter insures that the packet does not experience a gradient force. We analyze the interference pattern at a post-slit detection screen and find that it shares the predicted structure of a charged particle that is scattered by an AB magnetic flux tube.

In order to gain better understanding of this phenomenon, we introduce, in section III, a system that allows analytic solution. We calculate the partition func-

---

\* bernard@physics.unlv.edu

tion of a neutral spin-1/2 planar rotor placed in the aforementioned  $\vec{B}$  field configuration. In addition to verifying the AB features observed in our numerical demonstration, we conclude that a model characterized by a non-Abelian Wu-Yang[11] (WY) flux tube provides a more accurate description. We demonstrate that the, gauge invariant, partition function is an explicit function of the Wilson-loop[14] integral of a (WY) gauge field.

Early studies[15–18] have demonstrated how non-trivial gauge structures arise in molecular and atomic systems. In low energy atomic collisions[17, 19] and molecular structure[16] calculations, it is convenient to express the state vector in a basis of Born-Oppenheimer eigenstates. A complete set of such states leads to gauge potentials, coupled to the nuclear motion, that have both spatial and temporal components[17, 19, 20]. The spatial components describe a pure gauge, and its is only after truncation from a Hilbert space spanned by a complete set to a subspace that the spatial components acquire a non-trivial Wilson-loop value. For that reason it has sometimes been argued that gauge fields that lead to non-trivial Wilson loop integrals, (a.k.a geometric, or Berry, phases) are artifacts of the approximation or truncation procedure. In section IV, we investigate this question for the model introduced in section II. We demonstrate how an open ended, but gauge invariant, Wilson-line integral of a 3 + 1 gauge field along a space-time path can lead to a non-trivial spatial Wilson loop integral when projected to a closed path of the spatial subspace.

Wilczek and Zee[21] demonstrated how non-Abelian geometric phases arise in the slow evolution of a system possessing degenerate adiabatic eigenstates that are well separated from distant states. As our spin-1/2 model contains only two internal states, separated by an energy gap, the Wilczek-Zee mechanism is not applicable. Therefore we introduce, in section V, an extension to our two state model by positing a three-internal state system that allows analytic solutions. In the latter, two internal states are degenerate and a third state is separated from them by a large energy defect. We analyze its gauge structure, and show that higher order gauge corrections[17, 19, 22, 23] breaks the degeneracy evident in (semi-classical) adiabatic evolution[21]. As a consequence, gauge covariance is regained only in the 3+1 formalism[17]. In section VI, we provide a summary and conclusion of our efforts and propose possible systems in which the effects described above may be gleaned in a laboratory setting.

Unless otherwise stated we use units in which  $\hbar = 1$ . With the exception of the Pauli matrices, we use bold-face typeface to represent both vector and matrix valued quantities. In some cases, when there is the possibility of ambiguity, we use explicit vector notation to represent vector valued quantities.

## II. NUMERICAL DOUBLE-SLIT EXPERIMENT FOR A NEUTRAL SPIN-1/2 SYSTEM IN A STATIC MAGNETIC FIELD

Consider a neutral spin 1/2 atom or neutron with magnetic moment  $\boldsymbol{\mu}$ , and mass  $m$ , in the presence of a static background magnetic field

$$\vec{B} = B(\rho) \hat{\phi} + B_0 \hat{k} \quad (1)$$

where  $\phi, \rho$  are the polar and radial coordinates in a cylindrical coordinate system. We take  $B(\rho) \equiv B_\rho$ , and  $B_0$  to be constants so that  $\vec{B}$  describes a vortex configuration superimposed on a constant magnetic field in the  $\hat{k}$  direction. The Hamiltonian for a neutral spin-1/2 system is

$$H = -\frac{\hbar^2}{2m} \mathbb{1} \nabla_{\vec{R}}^2 + \boldsymbol{\mu} \vec{\sigma} \cdot \vec{B} \quad (2)$$

where  $\mathbb{1}$  is the unit  $2 \times 2$  matrix and  $\vec{\sigma}$  are Pauli matrices. The adiabatic, or BO, eigenenergies of  $H$  are the constant surfaces

$$V_{BO} = \pm \mu \sqrt{B_\rho^2 + B_0^2} \equiv \pm \Delta \quad (3)$$

separated by a finite energy gap  $2\Delta$ . Though the magnetic field lines have a vortex structure, and ignoring a small higher order correction[20], the gradient force  $-\vec{\nabla} V_{BO}$  vanishes. Thus wave packets evolve, as confirmed in a previous numerical study[20], with minimal distortion induced by the presence of scalar potentials.

Fig. (1) describes a wave packet, initially in the ground adiabatic state, whose probability density, as a function of time, is illustrated in the panels of that figure. In the first run of a simulation we set  $B_\rho = 0$  and the system evolves on the ground state adiabatic surface as the particle proceeds through the two slits. At the detection screen, shown by the red dashed line, the wave amplitude forms an interference pattern whose probability density is plotted in the left panel of Fig. (2). In that figure the solid blue line represents the data of this numerical simulation whereas the red dashed line is an analytic fit to the simulation. In calculating the latter we assumed that the probability amplitude at the observation screen is given by

$$\psi = \psi_R + \exp(i\beta) \psi_L \quad (4)$$

where  $\psi_{R,L}$  are amplitudes, based on a Huygens principle construction, due to contributions coming from the right and left slits, shown in Fig. (3), respectively.  $\beta$  is a measure of the relative phase between the amplitudes and for this run  $\beta \approx 0$  provides the best fit. On a second run we set  $B_0 = 0, B_\rho = |\Delta|$  so that the Zeeman energy splittings are unchanged from that of the first run. The resulting interference pattern is illustrated on the second (r.h.s) panel of Fig.(2) by the red line, and in that case we found the best value for  $\beta \approx \pi$ . In a subsequent

run we translated the  $\vec{B}$  field so that the vortex center, labeled  $x_c$  on the horizontal axis of Fig. (3), has been shifted to a point that is not framed by the pair of slits in the barrier. In that simulation we again found that  $\beta \approx 0$  provides the best fit to the numerical data. We also considered different ratios  $\tan \theta = B_\rho/B_0$  and fit  $\beta$  for these choices of  $\theta$ . The results are summarized by the following observations,

1. The data obtained in the simulations, for vortex centers  $-L/2 < x_c < L/2$ , are best described by Eq. (4) provided that  $\beta$  takes the value  $\pi(1 - \cos \theta)$ .
2. For an external magnetic field in which  $|x_c| > |L/2|$  the value  $\beta \approx 0$  provides the best fit.
3. If the packet mean kinetic energy  $E \gg 2\Delta$  the interference pattern is largely insensitive to the location of  $x_c$  and is best fit with  $\beta \approx 0$ .

The features described above are suggestive of dynamics influenced by topology. Indeed, it is the behavior predicted in Feynman's thought experiment treatment of Aharonov-Bohm (AB) scattering[1] of a charged scalar particle in a double slit apparatus[3]. Observations (1-3) are consistent with the following hypothesis,

$$\beta = \oint_C d\vec{s} \cdot \vec{A} \quad \text{where} \quad \vec{A} = \frac{(1 - \cos \theta)}{2\rho} \hat{\phi} \quad (5)$$

is a gauge potential that describes Aharonov-Bohm (AB)-like flux tube of strength  $(1 - \cos \theta)/2$  centered on the barrier at  $x_c = 0$ . The line integral is taken along a single circuit about a closed path  $C$  that circumscribes  $x_c = 0$  on the barrier.

Hamiltonian (2) possesses no overt gauge structure, but it is known [15–18] that effective gauge potentials can emerge in quantum systems not coupled to fundamental gauge fields. In this study we highlight the utility of using a gauge theory framework to characterize quantum systems that exhibit apparent topological AB-like behavior in a scattering setting. However, the features itemized above do not completely fit into the standard AB framework. It requires, as shown below, application of non-Abelian ideas and in order to elaborate on this observation we introduce a simpler physical system that allows an analytic description.

### III. THE SPIN-1/2 ROTOR; AN ANALYTIC TREATMENT.

We substitute the 2D kinetic energy operator, in Eq. (2),  $\frac{\hbar^2}{2m} \vec{\nabla}_R^2 \rightarrow \frac{1}{2I} \partial_\phi^2$  (setting  $\hbar = 1$ ) so that

$$H = -\frac{1}{2I} \mathbb{1} \partial_\phi^2 + \mu \sigma \cdot \vec{B}. \quad (6)$$

$H$  describes a neutral spin-1/2 particle constrained on a unit circle, ( i.e. a free rotor with spin and moment of inertia  $I$ ), subjected to an external magnetic given in

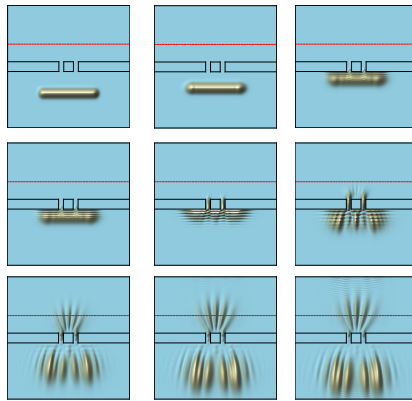


FIG. 1: Time series plot of wave packet at initial time  $t_0$  as it proceeds to, from left to right, to a double slit barrier (solid line outline). The red dashed line represent a detection screen, and at final time  $t_f$  shown in the panel at the lower right, the particle position is measured.

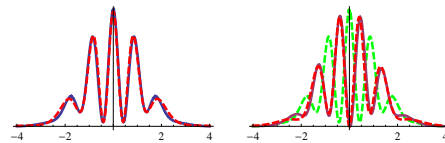


FIG. 2: Comparison of observed interference patterns at observation screen with a fit to model Eq. (4). Blue lines represent simulation data, red dashed lines represents fit to Eq. (4). The panel on the left corresponds to case where  $B_\rho = 0$  or  $\theta = 0$ . The panel on the right corresponds to case where  $\theta = \pi/2$  ( $B_0 = 0$ ), and the green line represents fringe patterns corresponding to  $\beta = 0$ .

Eq. (1). The rotor coordinates  $\phi = 0, 2\pi$  are identified. Hamiltonian Eq. (6) can be re-written as

$$\begin{aligned} H &= -\frac{1}{2I} \partial_\phi^2 + \mathbf{V} \\ \mathbf{V} &= \begin{pmatrix} \Delta \cos \theta & -i \exp(-i\phi) \Delta \sin \theta \\ i \exp(i\phi) \Delta \sin \theta & -\Delta \cos \theta \end{pmatrix}. \end{aligned} \quad (7)$$

$H$  commutes with

$$\mathbf{J} = -i \frac{\partial}{\partial \phi} + \frac{1}{2} \sigma_3 \quad (8)$$

whose eigenstates

$$\psi = \begin{pmatrix} \exp(i(m-1)\phi) c_1 \\ \exp(i m \phi) c_2 \end{pmatrix}, \quad (9)$$

where  $m$  is an integer, satisfy

$$\mathbf{J}\psi = (m - 1/2)\psi.$$

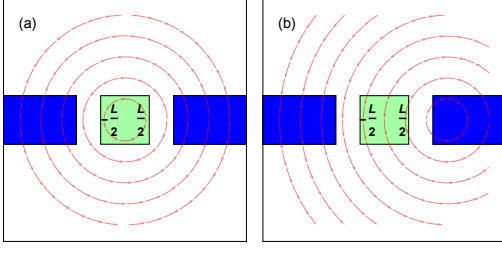


FIG. 3: Translation of magnetic field vortex center. Panel (a) vortex center  $x_c$  is situated at the center of the double-slit configuration. In Panel (b)  $x_c$  is translated to the right.

Using ansatz (9) we find that the eigenvalue equation  $(\mathbf{H} - E)\psi = 0$  reduces to

$$(\mathcal{H} - E)\underline{c} = 0$$

where  $\underline{c} \equiv \begin{pmatrix} c_1 \\ c_2 \end{pmatrix}$  and

$$\mathcal{H} = \left( \frac{m^2}{2I} + \frac{1-2m}{4I} \right) \mathbb{1} + \left( \frac{1-2m}{4I} + \Delta \cos \theta \right) \sigma_3 + \Delta \sin \theta \sigma_2. \quad (10)$$

$\mathbb{1}$  is the unit matrix and  $\sigma_2, \sigma_3$  are Pauli matrices. Introducing the unitary operator  $W = \exp(-i\sigma_1\Omega/2)$  where

$$\cos \Omega = \frac{\frac{(1-2m)}{4I} + \Delta \cos \theta}{\sqrt{\frac{(1-2m)^2}{16I^2} + \frac{(1-2m)\Delta \cos \theta}{2I} + \Delta^2}}$$

$$\sin \Omega = \frac{\Delta \sin \theta}{\sqrt{\frac{(1-2m)^2}{16I^2} + \frac{(1-2m)\Delta \cos \theta}{2I} + \Delta^2}}, \quad (11)$$

we find that

$$W\mathcal{H}W^\dagger = \left( \frac{m^2}{2I} + \frac{1-2m}{4I} \right) \mathbb{1} + \sqrt{\Delta^2 + \frac{(1-2m)^2}{16I^2} + \frac{(1-2m)\Delta \cos \theta}{2I}} \sigma_3 \quad (12)$$

Therefore,

$$\psi_\pm = \begin{pmatrix} \exp(i(m-1)\phi) & 0 \\ 0 & \exp(im\phi) \end{pmatrix} W^\dagger |\pm\rangle, \quad (13)$$

where

$$|+\rangle = \begin{pmatrix} 1 \\ 0 \end{pmatrix} \quad |-\rangle = \begin{pmatrix} 0 \\ 1 \end{pmatrix},$$

are eigenstates of  $\mathbf{H}$ . That is,

$$\mathbf{H}\psi_\pm(m) = E_\pm(m)\psi_\pm(m)$$

where

$$E_\pm = \frac{m^2}{2I} + \frac{(1-2m)}{4I} \pm \sqrt{\frac{(1-2m)^2}{16I^2} + \frac{(1-2m)\Delta \cos \theta}{2I} + \Delta^2} \quad (14)$$

In the limit  $\Delta \rightarrow 0$ , and for  $1-2m > 0$ ,  $\cos \Omega \rightarrow 1$ ,

$$\psi_+ \rightarrow \exp(i(m-1)\phi)|+\rangle \quad E_+ \rightarrow \frac{(m-1)^2}{2I}$$

$$\psi_- \rightarrow \exp(im\phi)|-\rangle \quad E_- \rightarrow \frac{m^2}{2I}, \quad (15)$$

likewise, for  $1-2m < 0$   $\cos \Omega \rightarrow -1$ , and

$$\psi_+ \rightarrow \exp(im\phi)|+\rangle \quad E_+ \rightarrow \frac{m^2}{2I}$$

$$\psi_- \rightarrow \exp(i(m-1)\phi)|-\rangle \quad E_- \rightarrow \frac{(m-1)^2}{2I}. \quad (16)$$

Eqs. (15,16) correspond to free rotor solutions.

In the limit  $\Delta \rightarrow \infty$ , provided that  $\Delta > \frac{|1-2m|}{4I}$ ,

$$E_+(m) \approx m^2 \left( \frac{1}{2I} + \frac{\sin^2 \theta}{8I^2 \Delta} \right) - m \left( \frac{(1+\cos \theta)}{2I} + \frac{\sin^2 \theta}{8I^2 \Delta} \right) + \Delta + \frac{1+\cos \theta}{4I} + \frac{\sin^2 \theta}{32I^2 \Delta} + \mathcal{O}\left(\frac{1}{\Delta^2}\right) \dots \quad (17)$$

and

$$E_-(m) \approx m^2 \left( \frac{1}{2I} - \frac{\sin^2 \theta}{8I^2 \Delta} \right) - m \left( \frac{(1-\cos \theta)}{2I} - \frac{\sin^2 \theta}{8I^2 \Delta} \right) - \Delta + \frac{1-\cos \theta}{4I} - \frac{\sin^2 \theta}{32I^2 \Delta} + \mathcal{O}\left(\frac{1}{\Delta^2}\right) \dots \quad (18)$$

### A. Adiabatic gauge

In order to gain insight into these solutions we transform the eigenvalue equation corresponding to Hamiltonian (7) into the so-called adiabatic representation [17] which we define by

$$\psi = U F \quad (19)$$

where

$$U \equiv \exp(-i\sigma_3\phi/2) \exp(i\sigma_1\theta/2) \exp(i\sigma_3\phi/2) \quad (20)$$

is a single-valued unitary operator. We get

$$-\frac{1}{2I}(\partial_\phi - i\mathbf{A})^2 F + \Delta \sigma_3 F = E F \quad (21)$$

where the non-Abelian, pure, gauge potential

$$\mathbf{A} = iU^\dagger \partial_\phi U = \frac{1}{2} \begin{pmatrix} \cos \theta - 1 & i \sin \theta \exp(-i\phi) \\ -i \sin \theta \exp(i\phi) & (1 - \cos \theta) \end{pmatrix}. \quad (22)$$

If we ignore the off-diagonal components of the gauge potential and project this equation to the ground manifold via projection operator  $|-\rangle\langle -|$ , we find

$$-\frac{1}{2I}(\partial_\phi - iA_g)^2 F_g + \frac{\beta}{2I} F_g - \Delta F_g = E F_g$$

$$A_g = 1/2(1 - \cos \theta) \equiv \alpha$$

$$\beta = A_{12}A_{21} = \sin^2 \theta/4 = \alpha(1 - \alpha). \quad (23)$$

We note that

$$F_g = \exp(im\phi) \quad (24)$$

is an eigenstate of Eq. (23) corresponding to eigenvalue

$$\begin{aligned} E_g &= \frac{(m-\alpha)^2}{2I} + \frac{(\alpha-\alpha^2)}{2I} - \Delta = \\ &= \frac{m^2}{2I} - \frac{m\alpha}{I} + \frac{\alpha}{2I} - \Delta. \end{aligned} \quad (25)$$

It agrees with the leading order limit of expression (18) as  $\Delta \rightarrow \infty$ ,

$$E_- = \frac{m^2}{2I} - \frac{m\alpha}{I} + \frac{\alpha}{2I} - \Delta = E_g, \quad (26)$$

Consider now the excited state manifold obtained via projection  $|+\rangle\langle+|$ .

$$F_e = \exp(i(m-1)\phi) \quad (27)$$

is an eigenstate of the latter corresponding to eigenvalue

$$\begin{aligned} E_e &= (m-1+\alpha)^2 + \frac{\beta^2}{4I} + V = \\ E_e &= \frac{m^2}{2I} + \frac{m(\alpha-1)}{I} + \frac{1-\alpha}{2I} \end{aligned} \quad (28)$$

Note that

$$1-\alpha = \frac{1}{2}(1+\cos\theta)$$

and so

$$E_e = \frac{m^2}{2I} - \frac{m(1+\cos\theta)}{2I} + \frac{1+\cos\theta}{4I} + \Delta \quad (29)$$

Or comparing to Eq. (17) we find, as  $\Delta \rightarrow \infty$ ,  $E_e = E_+$ .

In conclusion, we find that in the adiabatic gauge the following solutions to Eqs. (21) disregarding the off-diagonal couplings predicts adiabatic gauge eigen-solutions

$$\begin{aligned} \psi_g^a &= \exp(im\phi) \begin{pmatrix} 0 \\ 1 \end{pmatrix} \\ \psi_e^a &= \exp(i(m-1)\phi) \begin{pmatrix} 1 \\ 0 \end{pmatrix} \end{aligned} \quad (30)$$

with eigen-energies  $E_-, E_+$ , respectively. They agree with the leading order, in the limit  $\Delta \rightarrow \infty$ , eigenvalues obtained given by the exact analytic solutions to Eq. (7).

#### IV. THE WU-YANG FLUX TUBE.

Some time ago, T.T. Wu and C.N. Yang [11] entertained the notion of a non-Abelian Aharonov-Bohm effect. They postulated a non-Abelian flux tube that may allow, if found in nature, topological transformation of isotopic charge when a system, described by an isotopic

amplitude, is transported about the flux tube. In this paper we demonstrate how the spin-1/2 system described in the previous section possesses some of the salient features of a particle, with spin degrees of freedom, coupled to a Wu-Yang (WY) non-Abelian flux tube. To set the stage for that discussion we first introduce an idealized model in which a free rotor is coupled to a WY connection.

##### A. Rotor coupled to Wu-Yang gauge potential

Consider the following non-Abelian gauge potential

$$\begin{aligned} \mathbf{A} &= \sigma_3 \vec{A} \quad \vec{A} = \{A_x, A_y\} \\ A_x &= \frac{\alpha-y}{(x-x_0)^2+y^2} \quad A_y = \frac{\alpha(x-x_0)}{(x-x_0)^2+y^2} \end{aligned} \quad (31)$$

where  $x, y$  are the coordinates of a (iso) spin-1/2 particle.

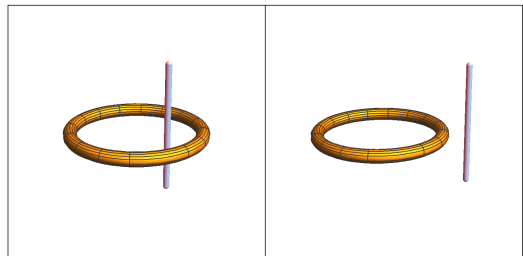


FIG. 4: Wu-Yang flux tube circumscribed by a rotor track (left panel). Right panel shows the flux tube exterior of the rotor track.

It is straightforward to verify that the spatial components of the matrix-valued curvature two-form  $\mathbf{F}$  vanish identically in the region excluding the point  $x = x_0 \geq 0, y = 0$ . From that observations it may appear that gauge connection (31) corresponds to that of a pure gauge. Nevertheless, as for the conventional AB vector potential, its Wilson loop integral circumscribing the point  $x_0, y = 0$  is non-trivial.

For connection (31) the gauge invariant trace of the Wilson loop phase integral has the value

$$W(C) \equiv \text{Tr} P \exp(-i \oint_C d\mathbf{s} \cdot \mathbf{A}) = 2 \cos 2m\pi\alpha \quad (32)$$

where  $C$  is an arbitrary contour (of counter-clockwise sense) that encloses the point  $(x_0, y = 0)$  and  $m$ , the winding number, itemizes the number of circuits taken around  $C$ .  $P$  represents path ordering.

As first pointed out by Wu and Yang, gauge potential (31) is a non-Abelian generalization of the Aharonov-Bohm potential. Despite the fact that in the gauge in which  $\mathbf{A}$  is diagonal and therefore has an ‘‘Abelianized’’ structure, it is not simply the potential of two AB flux tubes of opposite charge[24]. In this sense  $\mathbf{A}$  describes a non-Abelian flux tube piercing the  $xy$  plane at the point  $(x_0, y = 0)$

We seek a Schrödinger equation for a spin-1/2 particle, constrained on the unit circle  $x^2 + y^2 = 1$ , coupled to gauge potential (31), as well as a scalar potential  $\mathbf{A}_0 = -\sigma_3 \Delta$ , where  $\Delta$  is a constant energy defect. Constrained systems typically involve singular Lagrangians[25] and a rigorous derivation of the corresponding Hamiltonian requires application of Dirac's theory[25] of constrained dynamical systems. The latter has been applied to construct the quantum Hamiltonian of a scalar particle constrained on a circular path[26]. Here we use a more heuristic approach by considering the standard (unconstrained) Schrödinger equation in two dimensions and in which the spin-1/2 particle is minimally coupled to gauge potential (31). We have

$$-\frac{1}{2m}(\nabla - i\mathbf{A})^2\psi - \mathbf{A}_0\psi = i\frac{\partial\psi}{\partial t} \quad (33)$$

where

$$\vec{A} = -\hat{r} \frac{\alpha x_0 \sin(\phi)}{r^2 - 2rx_0 \cos(\phi) + x_0^2} + \hat{\phi} \frac{\alpha(r - x_0 \cos(\phi))}{r^2 - 2rx_0 \cos(\phi) + x_0^2} \quad (34)$$

is expressed in a polar coordinate system. If  $x_0 < r$ , and in the range  $-\pi < \phi \leq \pi$ , the function

$$\Omega_{>} = \alpha \frac{\phi}{2} - \alpha \arctan\left[\frac{r+x_0}{r-x_0} \tan\left(\frac{\phi}{2}\right)\right] \quad (35)$$

is single-valued and we are allowed the gauge transformation

$$\begin{aligned} \psi &\rightarrow \psi' = \exp(-i\Omega_{>}\sigma_3)\psi \\ \mathbf{A} &\rightarrow \mathbf{A}' = \mathbf{A} + \nabla\Omega_{>} = \hat{\phi} \frac{\alpha}{r}. \end{aligned} \quad (36)$$

Thus  $\mathbf{A}'$  describes a WY flux tube centered at the origin. If the particle is constrained to move on the unit circle and  $x_0 < 1$  we obtain the Schrödinger equation

$$\frac{1}{2I}(\partial_\phi - i\alpha\sigma_3)^2\psi' - \mathbf{A}_0\psi' = i\frac{\partial\psi'}{\partial t} \quad (37)$$

The energy eigenstates to Eq. (37) are

$$\begin{aligned} \psi'_m(E_+) &= \exp(im\phi) \begin{pmatrix} \frac{1}{\sqrt{2\pi}} \\ 0 \end{pmatrix} \\ E_+ &= \frac{(m+\alpha)^2}{2I} + \Delta \\ \psi'_m(E_-) &= \exp(im\phi) \begin{pmatrix} 0 \\ \frac{1}{\sqrt{2\pi}} \end{pmatrix} \\ E_- &= \frac{(m-\alpha)^2}{2I} - \Delta \end{aligned} \quad (38)$$

where  $m$  is an integer.

For  $x_0 > r$ ,  $\Omega_{>}$  is no longer single-valued but

$$\Omega_{<} = -\alpha \frac{\phi}{2} - \alpha \arctan\left[\frac{r+x_0}{r-x_0} \tan\left(\frac{\phi}{2}\right)\right] \quad (39)$$

is. Replacing  $\Omega_{>}$  with  $\Omega_{<}$  in (36) we find  $\mathbf{A}' = 0$ , i.e. a pure gauge. Thus, for  $x_0 > 1$  Eq. (37) is replaced with

$$\frac{1}{2I}\partial_\phi^2\psi' - \mathbf{A}_0\psi' = i\frac{\partial\psi'}{\partial t} \quad (40)$$

and,

$$\begin{aligned} \psi'_m(E_+) &= \exp(im\phi) \begin{pmatrix} \frac{1}{\sqrt{2\pi}} \\ 0 \end{pmatrix} \\ E_+ &= \frac{m^2}{2I} + \Delta \\ \psi'_m(E_-) &= \exp(im\phi) \begin{pmatrix} 0 \\ \frac{1}{\sqrt{2\pi}} \end{pmatrix} \\ E_- &= \frac{m^2}{2I} - \Delta. \end{aligned} \quad (41)$$

As the position of flux tube shifts from  $x_0 < 1$  to  $x_0 > 1$  the energy spectrum shifts into that of a free rotor. This topological feature is most clearly evident in the behavior of the partition function  $\mathcal{Z} = \sum_m \exp(-\beta E_m)$  where  $\beta$  is an inverse temperature and  $E_m$  are the energy eigenvalues for the eigenstates summarized above. Consider the propagator for Schrödinger Eq. (37) in the region  $|x_0| < 1$ ,

$$\begin{aligned} G(\phi t; \phi' t') &\equiv \langle \phi | \exp(-iH\tau) | \phi' \rangle = \\ &\sum_m \psi'_m(E_+, \phi) \psi'_m{}^\dagger(E_+, \phi') \exp(-iE_+\tau) + \\ &\sum_m \psi'_m(E_-, \phi) \psi'_m{}^\dagger(E_-, \phi') \exp(-iE_-\tau) \end{aligned} \quad (42)$$

where  $\tau = t - t'$ . Thus

$$\begin{aligned} G(\phi t; \phi' t') &= \frac{1}{2\pi} \exp(-i\frac{\alpha^2}{2I}\tau) \exp(-i\Delta\sigma_3\tau) \times \\ &\sum_m \exp(im(\phi - \phi')) \exp(-i\frac{m^2\tau}{2I}) \exp(-i\sigma_3 m \frac{\alpha\tau}{I}). \end{aligned} \quad (43)$$

With the following definition of the Jacobi-theta function [27, 28]

$$\theta_3(z, u) \equiv \sum_m \exp(i\pi m^2 u) \exp(2imz) \quad (44)$$

we re-express

$$\begin{aligned} G(\phi t; \phi' t') &\equiv \frac{1}{2\pi} \exp(-i\frac{\alpha^2}{2I}\tau) \exp(-i\Delta\sigma_3\tau) \times \\ &\begin{pmatrix} \theta_3(z_-, u) & 0 \\ 0 & \theta_3(z_+, u) \end{pmatrix} \end{aligned} \quad (45)$$

where

$$z_\mp = (\phi - \phi')/2 \mp \frac{\alpha\tau}{2I} \quad u = -\frac{\tau}{2\pi I}. \quad (46)$$

Employing the identity[27],

$$\begin{aligned} \theta_3(z, u) &= \frac{1}{\sqrt{-iu}} \exp(-i \frac{z^2}{\pi u}) \theta_3(-\frac{z}{u}, -\frac{1}{u}) = \\ &= \frac{\exp(\frac{-iz^2}{\pi u})}{\sqrt{-iu}} \sum_m \exp(-\frac{i\pi m^2}{u}) \exp(\frac{2imz}{u}) \end{aligned} \quad (47)$$

we re-write (45) as

$$\begin{aligned} G(\phi t; \phi' t') &= \sqrt{\frac{I}{2\pi i \tau}} \exp(-i\sigma_3 \Delta \tau) \sum_m \times \\ &= \exp\left(iI \frac{(2m\pi - \phi + \phi')^2}{2\tau}\right) \exp(i\alpha(2m\pi - \phi + \phi') \sigma_3). \end{aligned} \quad (48)$$

In this form, the propagator contains products that are proportional to the time interval  $\tau$ , and are of a dynamical origin, with factors that are independent of  $\tau$  and have a geometric, or topological, origin. Consider the classical equation of motion for a free rotor  $\phi(t) = \omega(t-t') + \phi'$  or, if we set  $t' = 0$ ,  $\phi(t) = \phi' + 2m\pi$ , for a rotor trajectory that encompass  $m$  circuits in a given time period  $\tau$ . The resulting classical action

$$S_m(\tau) = \int_0^\tau \frac{I}{2} \omega^2 = I \frac{(\phi - \phi' - 2m\pi)^2}{2\tau} \quad (49)$$

where we used the fact that  $\omega = (\phi - \phi' - 2m\pi)/\tau$ . Therefore,

$$\begin{aligned} G(\phi t; \phi' t') &= \sqrt{\frac{I}{2\pi i \tau}} \sum_m \exp(iS_m(\tau)) \exp(-i\sigma_3 \Delta \tau) \times \\ &= \exp(i\sigma_3 \alpha(2m\pi - \phi + \phi')). \end{aligned} \quad (50)$$

The partition function corresponds to the trace over all closed paths in which  $\phi = \phi'$ , and the time interval  $\tau$  is Wick rotated onto the imaginary axis. With the replacement  $\tau \rightarrow -i\beta$ , we obtain

$$\begin{aligned} \mathcal{Z}_{WY} &= \int_0^{2\pi} d\phi \text{Tr} G(\phi, -i\beta, \phi, 0) = \\ &= 2\sqrt{\frac{I}{2\pi\beta}} \cosh(\beta\Delta) \sum_m \exp(-\frac{2\pi^2 m^2 I}{\beta}) \cos(2m\pi\alpha). \end{aligned} \quad (51)$$

In the same manner we construct the partition function for  $x_0 > 1$ . Thus, we find

$$\begin{aligned} \mathcal{Z}_{WY} &= \mathcal{Z}_0 \sum_m \exp(-\frac{2\pi^2 m^2 I}{\beta}) \cos(2m\pi\alpha) \quad x_0 < 1 \\ \mathcal{Z}_{WY} &= \mathcal{Z}_0 \sum_m \exp(-\frac{2\pi^2 m^2 I}{\beta}) \quad x_0 > 1 \\ \mathcal{Z}_0 &\equiv 2\sqrt{\frac{I}{2\pi\beta}} \cosh(\beta\Delta). \end{aligned} \quad (52)$$

In expression (52) the partition function is expressed as a product of a purely dynamical contribution  $\mathcal{Z}_0$ , and

$$\begin{aligned} r_{\leq}(\beta) &\equiv 1 + \sum_{m=1}^{\infty} \exp(-\frac{2\pi^2 m^2 I}{\beta}) 2 \cos(2m\pi\alpha_{\leq}) \\ \alpha_{\leq} &= \alpha \quad x_0 < 1, \quad \alpha_{\leq} = 0 \quad x_0 > 1 \end{aligned} \quad (53)$$

which is modulated by a topological term  $\cos(2m\pi\alpha_{\leq})$  proportional to the trace of the Wilson loop integral (32) corresponding to winding number  $m$ .

In Fig (5) we plot the ratio  $r_{<}(\beta)$  as a function of the inverse temperature  $\beta$ . The graph illustrates significant variation of that ratio with respect to  $\alpha$  at lower temperatures. For  $x_0 > 1$ ,  $r(\beta)$  undergoes a phase change as

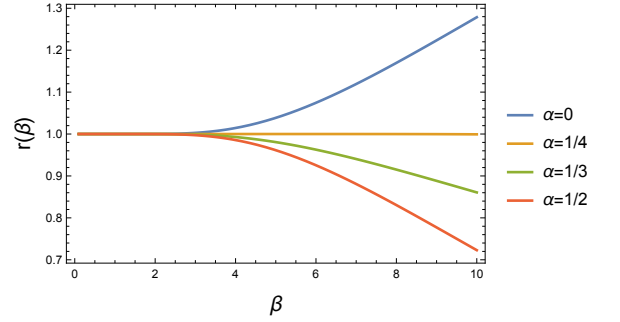


FIG. 5: Plot of the ratio  $r(\beta) \equiv \mathcal{Z}_{WY}/\mathcal{Z}_0$  as a function of  $\beta$ . The labeled curves correspond to different values of  $\alpha$ . We set the moment of inertia  $I = 1$ .

the curve is independent of variations in  $\alpha$ , and reverts to that labeled by  $\alpha = 0$  in that figure.

It is now instructive to compare the behavior of the gauge invariant partition function for the Wu-Yang flux tube with that of the system described by the partition function

$$\mathcal{Z} = \sum_m \exp(-\beta E_+) + \sum_m \exp(-\beta E_-) \quad (54)$$

where  $E_{\pm}$  are given by expression (14). The latter correspond to the partition function of our physical model; a neutral particle constrained on a rotor track in the presence of magnetic field (1).

Instead of comparing  $\mathcal{Z}_{WY}$  with  $\mathcal{Z}$ , we compare terms that only include the topological contribution to the partition functions. To that end we define

$$\tilde{r}(\beta) \equiv \mathcal{Z}/\tilde{\mathcal{Z}}_0 \quad (55)$$

where  $\tilde{\mathcal{Z}}_0$  is defined in (52) but modified by the contribution of the induced, scalar, counter term

$$\frac{\sin^2(\theta)}{8I} = \frac{\alpha(1-\alpha)}{2I}$$

introduced in Eqs. (25) and (28), i.e.

$$\tilde{\mathcal{Z}}_0 \equiv 2 \exp(-\beta \frac{(\alpha - \alpha^2)}{2I}) \sqrt{\frac{I}{2\pi\beta}} \cosh(\beta\Delta). \quad (56)$$



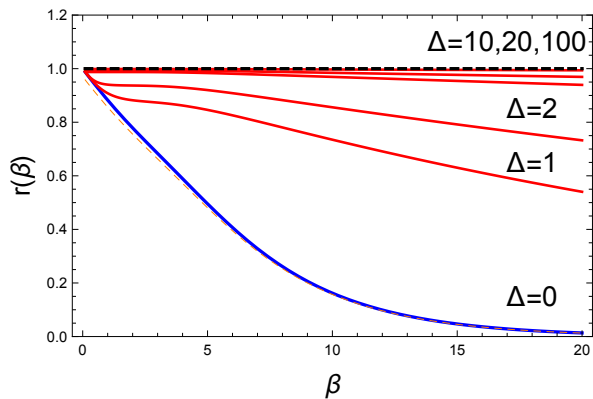


FIG. 6: Plot of the ratio  $\tilde{r}(\beta)$ , for different values of the energy defect  $\Delta$ , as a function of  $\beta$ . In this graph we chose the parameter values  $\alpha = 1/2, x_0 = 0, I = 1$ .

The ratio corresponding to the Wu-Yang system is given by the constant, black, dashed line. The red dashed line (superimposed by the blue line labeled  $\Delta = 0$ ) corresponds to a free rotor.

In Fig. (6) we plot the ratio  $r(\beta)$  for the values  $\alpha = 1/2, x_0 = 0$ , as a function of the inverse temperature  $\beta$  and the energy defect  $\Delta$ . The (blue) curve corresponding to energy defect  $\Delta = 0$  is identical to the curve obtained for the partition function of a free rotor (i.e. without a non-trivial gauge couplings). Since gauge potential (22) describes a pure gauge it is plausible that it does not contribute the value of the partition function  $\mathcal{Z}$ . However, for non-vanishing energy defects the graph shows a strong dependence of  $\mathcal{Z}$  on the topological factor  $\tilde{r}$ . For energy defect  $\Delta = 100$ , the value of  $\tilde{r}$  is almost identical to, at low temperatures ( $\beta \gg 1$ ), to the value predicted by the Wu-Yang flux tube given by expression (53) and shown by the dashed line in that figure. We conclude that for large values of  $\Delta$  the gauge invariant partition function for the system defined in Eq. (6) approaches that of particle coupled to Wu-Yang flux tube. Though gauge potential (22) is that of a pure gauge, the energy defect  $\Delta$  breaks a restricted spacial gauge symmetry as it corresponds to the time component of a 3+1 gauge field[17]. Consequently we find a non-trivial, non-Abelian, Wilson loop contribution to the partition function. If we restrict our attention to the ground state, the latter appears as an Abelian holonomy whose semiclassical analog (in which the quantum variable  $\phi$  is demoted to a classical parameter  $\phi(t)$ ) corresponds to Berry's geometric phase[29, 30].

Let's define amplitude  $G$ , so that

$$\psi = U \exp(-i\sigma_3 \Delta t)G \quad (57)$$

where  $U$  is defined in Eq. (20). Inserting (57) into the time dependent version of Eq. (21), we obtain

$$-\frac{1}{2I}(\partial_\phi - i\mathbf{A}(t))^2 G = i \frac{\partial G}{\partial t} \quad (58)$$

where

$$\mathbf{A}(t) = \frac{1}{2} \begin{pmatrix} \cos \theta - 1 & i \sin \theta \exp(-i\phi(t)) \\ -i \sin \theta \exp(i\phi(t)) & (1 - \cos \theta) \end{pmatrix} \quad (59)$$

$$\phi(t) \equiv \phi - 2 \Delta t.$$

$\mathbf{A}(t)$ , like  $\mathbf{A}$  in Eq. (22), is a pure gauge and generates a trivial Wilson loop integral. However, if we replace the off-diagonal components of (59) with a time expectation value, over interval  $\tau$ ,

$$\pm i \sin \theta \langle \exp(\mp i\phi(t)) \rangle \approx \pm i \sin \theta \langle \exp(\mp i\phi) \rangle \mathcal{O}\left(\frac{1}{\tau \Delta}\right)$$

which as  $\Delta \rightarrow \infty$  we ignore. In this approximation pure gauge  $\mathbf{A}(t)$  is replaced with the gauge potential of a non-Abelian WY flux tube.

## B. Shifted magnetic vortex field

In the previous section we demonstrated how, in the limit  $\Delta \rightarrow \infty$ , the eigen-solutions to Hamiltonian (6) tend to those described by an effective Hamiltonian containing a Wu-Yang flux tube. Suppose we have the following  $\mathbf{B}$  field configuration

$$\mathbf{B}/B_0 = \frac{-y \hat{\mathbf{i}}}{\sqrt{(x-x_0)^2 + y^2}} + \frac{(x-x_0) \hat{\mathbf{j}}}{\sqrt{(x-x_0)^2 + y^2}} \quad (60)$$

which describes a vortex configuration centered at  $(x = x_0, y = 0)$ . The Hamiltonian in (2)  $\mu \boldsymbol{\sigma} \cdot \mathbf{B}$  is given by

$$\begin{pmatrix} 0 & \frac{i\Delta(x_0-x+iy)}{\sqrt{(x_0-x)^2+y^2}} \\ -\frac{i\Delta(x_0-x-iy)}{\sqrt{(x_0-x)^2+y^2}} & 0 \end{pmatrix} \quad (61)$$

$$\Delta = \mu B_0$$

and replacing  $x \rightarrow \cos \phi, y \rightarrow \sin \phi$  the above expression can be re-written as

$$\begin{pmatrix} 0 & -i\Delta e^{-i\Omega(\phi)} \\ i\Delta e^{i\Omega(\phi)} & 0 \end{pmatrix} \quad (62)$$

$$\tan \Omega = \frac{\sin \phi}{\cos \phi - x_0}$$

Now if we define the operator

$$U = \exp(-i\sigma_3 \Omega/2) \exp(i\sigma_1 \pi/4) \exp(i\sigma_3 \Omega/2) \quad (63)$$

we find that

$$H = U H_{BO} U^\dagger$$

$$H_{BO} = \begin{pmatrix} \Delta & 0 \\ 0 & -\Delta \end{pmatrix} \quad (64)$$

Forming the non-Abelian connection  $A \equiv iU^\dagger \frac{\partial}{\partial \phi} U$  we find,

$$A = \frac{1 - x_0 \cos \phi}{2 + 2x_0^2 - 4x_0 \cos \phi} \begin{pmatrix} -1 & i \exp(-i\Omega) \\ -i \exp(i\Omega) & 1 \end{pmatrix} \quad (65)$$



The diagonal components of  $A_d$  of  $A$  has the form,

$$A_d = \sigma_3 \frac{x_0 \cos \phi - 1}{2x_0^2 - 4 \cos \phi x_0 + 2} \quad (66)$$

and for the special case  $x_0 = 0$  reduces to  $A_d = \sigma_3/2$  and describes the non-Abelian Wu-Yang flux tube of “charge”  $1/2$  centered at the origin. In Fig. (7) we plot, with the red solid lines, the energy spectrum calculated for Hamiltonian (6) using field (60) for values of  $x_0$  ranging from  $x_0 = 0$  to  $x_0 = 1.8$ . Superimposed on the figure, by the blue dotted lines, is the corresponding spectrum for a rotor system minimally coupled to the gauge field of a Wu-Yang flux tube centered at  $x_0$ , and calculated using the analytic formulas given in Eqs. (38) and (41). The dashed blue lines correspond to the eigenvalues for a free planar rotor.

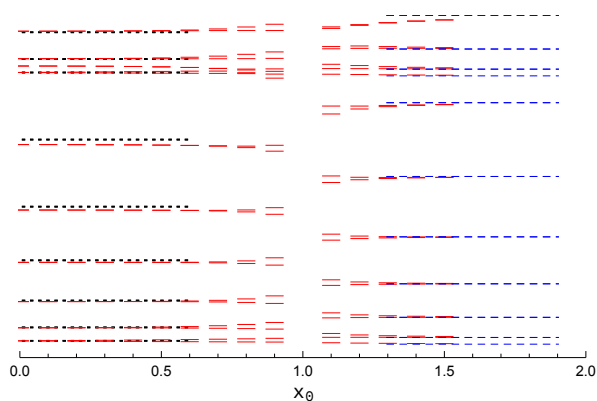


FIG. 7: Energy spectrum for the rotor as a function of the vortex origin. For  $x_0 < 1$ , it is circumscribed by the rotor track. Discontinuity at  $x_0 = 1$ , demonstrates evidence of a topological phase transition.

## V. THE IMPORTANCE OF BEING NON-ABELIAN

Consider the Schrödinger equation for a spin-1/2 particle of mass  $m$

$$\begin{aligned} -\frac{1}{2m}(\nabla - i\vec{A}')^2\psi - \mathbf{A}'_0(\phi)\psi &= i\frac{\partial\psi}{\partial t} \\ \mathbf{A}'_0(\phi) &= \exp(-i\mathbf{a}\phi)\Delta\exp(i\mathbf{a}\phi) \\ \Delta &\equiv -\Delta\sigma_3, \end{aligned} \quad (67)$$

where  $\mathbf{a}$  is a constant  $2 \times 2$  hermitian matrix,  $\phi$  is the azimuthal angle in a cylindrical coordinate system and  $\vec{A}'$ ,  $\mathbf{A}'_0$  are the spatial and time components of a 3+1 matrix-valued (i.e. non-Abelian) gauge potential. Let  $\vec{A}' = 0$ , and so Eq. (67) describes a spin-1/2 particle coupled to a matrix, or spin-dependent, scalar potential  $-\mathbf{A}'_0$ . With gauge transformation  $\psi = \mathbf{U}F$ ,

$\mathbf{U} = \exp(-i\mathbf{a}\phi)$ , amplitude  $F$  obeys,

$$-\frac{1}{2m}(\nabla - i\vec{A})^2F - \mathbf{A}_0(\phi)F = i\frac{\partial F}{\partial t} \quad (68)$$

where

$$\begin{aligned} \vec{A} &= \mathbf{U}^\dagger \vec{A}' \mathbf{U} + i\mathbf{U}^\dagger \nabla \mathbf{U} = \frac{\mathbf{a}}{\sqrt{x^2 + y^2}} \hat{\phi} \\ \mathbf{A}_0 &= \mathbf{U}^\dagger \mathbf{A}'_0 \mathbf{U} + i\mathbf{U}^\dagger \frac{\partial \mathbf{U}}{\partial t} = \Delta \end{aligned} \quad (69)$$

The similarity of Eq. (67) with (68) is a reflection of the fact that the Schrödinger equation is covariant, or form invariant, with respect to gauge transformations. Observable quantities, the eigenvalues of operators, are gauge invariant.

Now gauge transformation  $\mathbf{U}(\phi) = \exp(-i\mathbf{a}\phi)$  must be single-valued, i.e.  $\mathbf{U}(0) = \mathbf{U}(2\pi)$ , and so  $\mathbf{a}$  has the form

$$\mathbf{a} = \mathbf{Z}^\dagger \begin{pmatrix} m & 0 \\ 0 & n \end{pmatrix} \mathbf{Z} \quad (70)$$

where  $m, n$  are integers,  $\theta, \gamma$  are constants, and

$$\mathbf{Z} = \exp(i\theta\sigma_2/2) \exp(-i\gamma\sigma_3/2)$$

is a constant unitary matrix. For the sake of simplicity, we consider the case  $n = -m$  and so

$$\mathbf{a} = q \begin{pmatrix} \cos \theta & \exp(i\gamma) \sin \theta \\ \exp(-i\gamma) \sin \theta & -\cos \theta \end{pmatrix}, \quad (71)$$

where  $q$  is an integer and  $\theta, \gamma$  are parameters, satisfies Eq. (70). A full quantum description of this model is given in Appendix A, but here we first explore the behavior of the Wilson loop integral of the 3+1 gauge potentials  $\mathbf{a}, \mathbf{A}_0$ .

Consider the following path-ordered Wilson-loop integral,

$$\begin{aligned} \mathbf{W}(C_0) &= P \exp(i \int_{C_0} d\vec{R} \cdot \vec{A}) = \\ &= \exp(i\mathbf{a} \int d\phi) \end{aligned} \quad (72)$$

where we used  $\vec{A}$  defined in Eq. (69),  $C_0$  is a closed path that circumscribes the origin in the,  $z = 0, xy$  plane and  $d\phi$  is the differential angle, with respect to the origin, of a segment of an arc along the path. Since  $\int d\phi = 2\pi m$ , where  $m$  is the winding number of the path,

$$\begin{aligned} \mathbf{W}(C_0) &= \exp(i\mathbf{a} 2\pi m) = \\ &= \mathbf{Z}^\dagger \exp(i 2\pi q m \sigma_3) \mathbf{Z} = \mathbb{1}. \end{aligned} \quad (73)$$

This identity is simply a reflection of the fact that  $\vec{A}$  is a pure gauge.

### A. Wilson line in space-time.

In our discussion so far we noted that the partition function of our spin-1/2 systems contain Wilson loop contributions that arise from non-trivial gauge fields, despite the fact that the spatial components  $\vec{\mathbf{A}}$  of the 3+1 gauge potentials describe a pure gauge.

To achieve a better understanding of how non-trivial Wilson loop contributions arise in systems that are putatively coupled to a pure gauge, we note that in evaluation of the partition function we need to take into account paths in space and time. Therefore, we consider a general path integral along an arbitrary path (not including the origin)  $C(a, b)$  from point  $a$  to  $b$  for gauge field  $\mathbf{A}_\mu$ . Here  $\mu$  is an index that identifies a space-time component

$$\mathbf{A}_\mu = \{\mathbf{A}_0, \mathbf{A}_x, \mathbf{A}_y, \mathbf{A}_z\} \quad \mu = 0, 1, 2, 3$$

and we use a summation convention so that

$$\begin{aligned} \mathbf{W}(a, b) &\equiv P \exp\left(i \int_{C(a,b)} dz^\mu \mathbf{A}_\mu\right) \\ dz^\mu \mathbf{A}_\mu &\equiv dt A_0 + \vec{\mathbf{A}} \cdot d\vec{\mathbf{R}} \end{aligned} \quad (74)$$

With gauge transformation  $\psi = \mathbf{U}\psi'$ , the gauge potentials[14]

$$\begin{aligned} \mathbf{A}_\nu &\rightarrow \mathbf{A}'_\nu = \mathbf{U}^\dagger \mathbf{A}_\nu \mathbf{U} + i \mathbf{U}^\dagger \partial_\nu \mathbf{U}, \quad \nu = 1, 2, 3 \\ \mathbf{A}_0 &\rightarrow \mathbf{A}'_0 = \mathbf{U}^\dagger \mathbf{A}_0 \mathbf{U} + i \mathbf{U}^\dagger \partial_t \mathbf{U} \\ \mathbf{W}(a, b) &\rightarrow \mathbf{U}^\dagger(b) \mathbf{W}(a, b) \mathbf{U}(a). \end{aligned} \quad (75)$$

Consider paths of the type illustrated in Fig. (8). They are trajectories in a manifold that is a Cartesian product of the coordinates in the  $xy$  plane with a 1-dimensional manifold labeled by time  $t$ . The trace of  $\mathbf{W}(a, b)$  for an open-ended path is not, in general, gauge invariant. However, we evaluate the integral only along paths in which the projection of coordinates  $a, b$  onto the spatial plane are equal at the initial and final points of the trajectory. We also limit the gauge group to time independent gauge transformations  $\mathbf{U}$  so that the trace of  $\mathbf{W}(a, b)$  is invariant under this group of transformations. Below we study the properties of  $\mathbf{W}(a, b)$  as a function of the defect parameter  $\Delta$ .

We parameterize the trajectory  $z(\tau)$

$$z(\tau) = x(\tau)\hat{\mathbf{i}} + y(\tau)\hat{\mathbf{j}} + f_t(\tau)\hat{\mathbf{k}} \quad (76)$$

where  $\hat{\mathbf{i}}, \hat{\mathbf{j}}$  are the basis vectors in the spatial plane, and  $\hat{\mathbf{k}}$  is the unit vector orthogonal to that plane and which we take to define the time axis, so that the physical time  $t \equiv f_t(\tau)$ . The functions  $x(\tau), y(\tau), f_t(\tau)$  are arbitrary but satisfy the conditions  $x(0) = x(t_f), y(0) = y(t_f)$  where  $0 < \tau \leq t_f$  in order for the path to make a closed loop, in the  $xy$  plane at  $\tau = t_f$ . Using Eqs. (69,74,76) we get

$$\begin{aligned} \mathbf{W}(a, b) &= P \exp\left(i \int_{C(a,b)} dz^\mu \mathbf{A}_\mu\right) = \\ T \exp\left(i \int_0^{t_f} d\tau \left(\frac{d\phi}{d\tau} \mathbf{a} + \frac{df_t}{d\tau} \Delta\right)\right) \end{aligned} \quad (77)$$

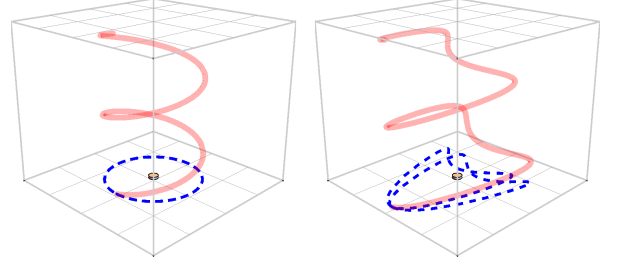


FIG. 8: Space-time paths for the Wilson line integral (74). Deformations within a set of projected paths on the  $xy$  plane, shown by the dashed lines, that share the same winding number about the origin do not alter the value of the integral.

where  $T$  denotes time-ordering. If  $\mathbf{a}$  commutes with  $\Delta$  expression (77) factors into a product of the trivial Wilson-loop integral (72) and a dynamical contribution generated by  $\mathbf{A}_0$ . For gauge potential (71) such a factorization is not possible, as  $[\mathbf{a}, \sigma_3] \neq 0$ . However, integral (77) can easily be evaluated for a class of paths where  $d\phi/dt \equiv \omega$  is constant. Since

$$\frac{d\phi}{dt} = \frac{d\phi}{d\tau} \frac{1}{f'_t(\tau)}$$

and  $\phi(t_f) = \phi(0) \text{ Mod}(2\pi)$

$$\begin{aligned} \mathbf{W}(a, b) &= T \exp\left(i \int_0^{t_f} d\tau \frac{d\phi}{d\tau} \left(\mathbf{a} + \frac{\Delta}{\omega}\right)\right) = \\ \exp\left(i 2\pi m \left(\mathbf{a} + \frac{\Delta}{\omega}\right)\right), \end{aligned} \quad (78)$$

where  $m$  is the winding number of the path. Exponentiation of expression (78) results in

$$\begin{aligned} \mathbf{W}(a, b) &= \\ \cos(2\pi m \Omega) \mathbb{1} - i \frac{(\Delta/\omega - q \cos \theta)}{\Omega} \sin(2\pi m \Omega) \sigma_3 + \\ i \frac{q \sin \theta}{\Omega} \sin(2\pi m \Omega) (\cos \gamma \sigma_1 - \sin \gamma \sigma_2). \end{aligned} \quad (79)$$

where

$$\Omega = \frac{\sqrt{\Delta^2 + q^2 \omega^2 - 2\Delta q \omega \cos \theta}}{\omega}. \quad (80)$$

Let's define an effective vector potential

$$\mathcal{A}_{eff} \equiv \frac{\hat{\phi}}{\sqrt{x^2 + y^2}} \left(\mathbf{a} + \frac{\Delta}{\omega}\right). \quad (81)$$

Unlike the pure gauge  $\vec{\mathbf{A}}$ , defined in Eq. (69),  $\mathcal{A}_{eff}$  engenders a non-trivial Wilson loop integral  $\mathcal{W}_C$  for any loop, in the  $z = 0$  plane, enclosing the origin. Indeed,

$$\mathbf{W}(a, b) = \mathcal{W}_C = \oint_C d\vec{\mathbf{R}} \cdot \mathcal{A}_{eff} \quad (82)$$

where  $C$  is the projection of the space-time path (76) onto the  $xy$  plane. Because  $x(0) = x(t_f), y(0) = y(t_f)$ ,  $C$  forms a closed loop.

In summary, we demonstrated how the space-time open-ended path integral of a 3 + 1 non-Abelian gauge potential leads to a non-trivial Wilson loop integral of an effective gauge field  $\mathcal{A}_{eff}$ . For time independent gauge transformations, the trace of  $\mathbf{W}$  is gauge invariant. As  $\mathcal{W}_C$  depends only on the winding number,  $C$  can be shrunk to an infinitesimal loop about the origin without altering the value of  $\mathcal{W}_C$ . Thus  $\mathcal{A}$  represent the gauge potential of a Wu-Yang flux tube of "charge"  $\pm\Omega$ , the eigenvalues of  $\mathbf{a} + \frac{\Delta}{\omega}$ . In general,  $\mathbf{W}(a, b)$  is a function of the dynamical parameters,  $\Delta, \omega$ , but for large  $\frac{\Delta}{\omega} \gg 1$ , it tends to the product

$$\mathbf{W}(a, b) \rightarrow \exp\left(-\frac{2im\pi}{\omega}\sigma_3\right) \exp(2im\pi q \cos\theta \sigma_3) + \mathcal{O}(\omega/\Delta) \quad (83)$$

We evaluated  $\mathbf{W}$  in the adiabatic gauge[17], wherein  $\mathbf{A}_0$  is diagonal. Because  $\mathbf{U}(\phi = 0) = \mathbf{U}(\phi = 2\pi) = \mathbb{1}$ ,  $\mathbf{W}$  is invariant under a gauge transformation into the diabatic gauge[17]. The latter corresponds to Schrödinger Eq. (67) in which the spatial component  $\mathbf{A}' = 0$ . In that gauge

$$\begin{aligned} \mathbf{W}(a, b) &= P \exp\left(i \int_{C(a,b)} dz^\mu \mathbf{A}'_\mu\right) = \\ T \exp\left(i \int_0^{t_f} d\tau \frac{df_t}{d\tau} \mathbf{A}'_0(\phi(\tau))\right) &= \\ T \exp\left(i \int_0^{\frac{2\pi m}{\omega}} dt \exp(i\mathbf{a}\omega t) \mathbf{\Delta} \exp(-i\mathbf{a}\omega t)\right) & \quad (84) \end{aligned}$$

where we used the fact that  $f_t(\tau) = t$  and  $\phi(t) = \omega t$ . Replacing the upper limit in integral (84) with an arbitrary time value  $t$ , we find that  $\mathbf{W}(t)$  obeys a time dependent Schrödinger equation.

$$\begin{aligned} i \dot{\mathbf{W}}(t) &= \mathcal{H}(t) \mathbf{W}(t) \\ \mathcal{H}(t) &= \exp(i\mathbf{a}\omega t) \mathbf{\Delta} \exp(-i\mathbf{a}\omega t). \end{aligned} \quad (85)$$

It can be integrated to give

$$\mathbf{W}(t) = \exp(-i\mathbf{a}\omega t) \exp\left(i\omega t \left(\mathbf{a} + \frac{\Delta}{\omega}\right)\right). \quad (86)$$

Thus,

$$\mathbf{W}(a, b) = \mathbf{W}\left(t = \frac{2\pi m}{\omega}\right)$$

where we used the fact that  $\exp(2i\pi m \mathbf{a}) = \mathbb{1}$ . In the adiabatic limit as  $\omega \rightarrow 0$ ,  $\mathbf{W}(a, b)$  tends to the limit Eq. (83). In that expression, the first, dynamical, factor  $\exp\left(-\frac{2im\pi}{\omega}\sigma_3\right)$  depends on the length of time  $t_f = 2\pi m/\omega$  that it takes for the system to travel from starting to end points. The second factor

$$\exp(2im\pi q \cos\theta \sigma_3)$$

depends on spatial path taken. This factorization is in harmony with the adiabatic theorem[29].

## VI. ON THE WILCZEK-ZEE MECHANISM

In the previous sections we illustrated how non-trivial gauge structures arise in a vector space that is a direct product of a two-state (or qubit) system with the Hilbert space of a rotor. It is straightforward to extend this formalism to systems possessing additional internal degrees of freedom (e.g. spin-1 etc.). Indeed, this procedure is ubiquitous in theoretical studies of slow atomic collisions and non-adiabatic molecular dynamics. In those applications it is especially applicable if the total system energy  $E \ll \Delta$  where  $\Delta$  is an energy defect that separates a sub-manifold of Born-Oppenheimer (BO) states separated by a large energy gap from energetically higher lying BO states. Thus the Hilbert space amplitude is projected to a set of effective, or matrix-valued, amplitudes in the sub-space. The resulting set of coupled equations constitute the Born-Huang[31] approximation, or the method of Perturbed Stationary States[32] (PSS). The latter typically result in effective, non-trivial, non-Abelian gauge couplings among the sub-space amplitudes.

In a quasi-classical version of this procedure, Wilczek and Zee demonstrated how the projected amplitudes, for a sub-manifold of degenerate energy eigen-states, acquire a non-Abelian geometric phase during adiabatic evolution.

Below we consider a spin-1 rotor system in which two internal states possess degenerate energy eigenvalues that are separated from the remaining internal states by a large energy gap  $\Delta$ . To illustrate this mechanism we choose a straightforward extension of Hamiltonian (67)

$$\begin{aligned} H &= -\frac{1}{2I} \partial_\phi^2 + \mathbf{U}(\phi) \mathbf{V} \mathbf{U}^\dagger(\phi) \\ \mathbf{U} &= \exp(-i\mathbf{a}\phi) \\ \mathbf{a} &= \begin{pmatrix} 0 & \frac{\sin\theta}{\sqrt{2}} & -\frac{\sin\theta}{\sqrt{2}} \\ \frac{\sin\theta}{\sqrt{2}} & \cos\theta & 0 \\ -\frac{\sin\theta}{\sqrt{2}} & 0 & -\cos\theta \end{pmatrix} \\ \mathbf{V} &= \begin{pmatrix} \Delta & 0 & 0 \\ 0 & e_g & 0 \\ 0 & 0 & e_g \end{pmatrix} \end{aligned} \quad (87)$$

This particular choice for  $\mathbf{a}$  guarantees that  $\mathbf{U}$  is single-valued. For our purposes it is convenient to choose  $e_g = -\sin^2\theta/4I$ .

Defining the adiabatic gauge amplitude  $F$ , so that

$$\psi = \mathbf{U} F$$

we obtain the matrix-valued Schrödinger equation

$$-\frac{1}{2I} (\partial_\phi - i\mathbf{a})^2 F + \mathbf{V} F = i \frac{\partial F}{\partial t} \quad (88)$$

With ansatz

$$F = \exp(im\phi) \exp(-iEt) \mathbf{c} \quad (89)$$

where  $\mathbf{c}$  is a constant column matrix, we are led to the eigenvalue equation  $\det|\mathbf{h} - \mathbb{1} E| = 0$  where

$$\mathbf{h} = \frac{(\mathbb{1} m - \mathbf{a})^2}{2I} + \mathbf{V} \quad (90)$$

Finding the eigenvalues of  $\mathbf{h}$  involve solving for the roots of a cubic equation and for which analytic expressions, the Cardano formula, is available. The latter can be used to construct the gauge invariant partition function

$$\mathcal{Z} \equiv \sum_{i=1}^3 \sum_m \exp(-\beta E_m^i). \quad (91)$$

to the required degree of accuracy. The sums extend over the spectrum of  $\mathbf{h}$ , which are itemized by the motional quantum number  $m$ , as well as the internal state quantum number  $i$ . Here  $\beta$  is an inverse temperature.

Instead, because  $\Delta \gg e_g$ , we use the PSS approximation in which the amplitude  $F$  is projected to a Hilbert subspace. In this case, the subspace is spanned by the degenerate eigen-states of  $\mathbf{V}$ , or the computational basis for a single qubit. Introducing the projection operator

$$P \equiv \begin{pmatrix} 0 & 0 & 0 \\ 0 & 1 & 0 \\ 0 & 0 & 1 \end{pmatrix}$$

defining

$$G = P F$$

we obtain the PSS equations

$$-\frac{1}{2I}(\partial_\phi - i \mathbf{a}_p)^2 G + P \frac{\mathbf{a} \cdot \mathbf{a} - \mathbf{a}_p \cdot \mathbf{a}_p}{2I} G + \mathbf{V}_p G = i \frac{\partial G}{\partial t} \quad (92)$$

where  $\mathbf{a}_p \equiv P \mathbf{a} P$ ,  $\mathbf{V}_p = P \mathbf{V} P$ . In this approximation we ignore couplings between the  $P$  and  $Q = \mathbb{1} - P$  sub-manifolds.

Though  $V_p$  is diagonal and degenerate, the higher order induced scalar term[19, 22]

$$P \frac{\mathbf{a} \cdot \mathbf{a} - \mathbf{a}_p \cdot \mathbf{a}_p}{2I} P = \frac{1}{4I} \begin{pmatrix} 0 & 0 & 0 \\ 0 & \sin^2 \theta & -\sin^2 \theta \\ 0 & -\sin^2 \theta & \sin^2 \theta \end{pmatrix} \quad (93)$$

is not. An additional gauge transformation in the projected qubit subspace  $G = \mathbf{W} G'$  results in

$$-\frac{1}{2I}(\partial_\phi - i \mathbf{a}'_p)^2 G' + \mathbf{V}'_p G' = i \frac{\partial G'}{\partial t} \\ \mathbf{a}'_p = \cos \theta \sigma_1 \\ \mathbf{V}'_p = \frac{\sin^2 \theta}{4I} \sigma_3 \\ \mathbf{W} = \exp(-i \sigma_2 \pi / 4) \quad (94)$$

where  $\sigma_i$  are the standard spin-1/2 Pauli matrices.

Because the eigen-states of  $\mathbf{V}'_p$  are not degenerate, Eq. (94) is no longer covariant under a Wilczek-Zee gauge transformation. In the latter formulation  $\phi(t)$  is treated as a classical variable undergoing adiabatic evolution. Here  $\phi$  is a quantum variable, and the symmetry responsible for the degeneracy in a quasi-classical formulation is broken. However we can, as described in the previous sections, enlarge the gauge group by allowing the (matrix) scalar potential to be treated as the time component of a 3 + 1 gauge potential.

Consider the gauge potential.

$$\mathbf{A}'_p = \sigma_1 \cos \theta \left( \frac{-\hat{\mathbf{i}} y}{x^2 + y^2} + \frac{\hat{\mathbf{j}} x}{x^2 + y^2} \right) \quad (95)$$

which begets  $\mathbf{a}'_p$  in Eq. (94). Its Wilson loop integral for a path  $C$  circumscribing the origin assumes the value

$$\mathcal{W}_C(m) \equiv \text{Tr} P \exp(i \oint_C d\mathbf{r} \cdot \mathbf{A}'_p) = 2 \cos(2\pi m \cos \theta) \quad (96)$$

where  $m$  is the winding number. For values  $\cos \theta \notin \mathbb{Z}$ , identity (96) demonstrates that  $\mathbf{a}'_p$ , unlike  $\mathbf{a}$  in Eq. (70), is not a pure gauge. The energy eigenvalues associated with Eq. (94) are

$$E = e_0 \pm e_1 \\ e_0 = \frac{m^2 + \cos^2 \theta}{2I} \quad e_1 = \frac{1}{I} \sqrt{\frac{\sin^4 \theta}{16} + m^2 \cos^2 \theta} \quad (97)$$

and so the reduced partition function

$$z = 2 \sum_m \exp(-\beta e_0) \cosh(\beta e_1). \quad (98)$$

For higher temperatures, or  $\beta \ll 1$ , we can approximate

$$e_1 \approx \frac{|m|}{I} \cos \theta$$

which implies that

$$z \approx 2 \sum_m \exp(-\beta \frac{m^2 + \cos^2 \theta}{2I}) \cosh(\beta \frac{m \cos \theta}{I}) \quad (99)$$

Applying a Poisson transformation, we get

$$z \approx 2 \sqrt{\frac{2\pi I}{\beta}} \sum_m \exp(-\frac{2I m^2 \pi^2}{\beta}) \cos(2\pi m \cos \theta) \quad (100)$$

In order to obtain the total partition function  $\mathcal{Z}$ , we must include the contribution from the distant state whose energy eigenvalue  $E_m^{i=1} \gg e_0 \pm e_1$ . In solving for the eigenvalues of  $\mathbf{h}$  we find that

$$E_m^{i=1} = \frac{m^2}{2I} + \frac{\sin^2 \theta / 2}{2I} + \Delta + \mathcal{O}\left(\frac{1}{\Delta}\right) + \dots \quad (101)$$

and so the leading order contribution is dominated by the term  $\exp(-\beta \Delta) \rightarrow 0$  as  $\Delta \rightarrow \infty$ . Therefore,

$$\mathcal{Z} \approx z = \sqrt{\frac{2\pi I}{\beta}} \sum_k \exp(-S_0(k)) \cos(\mathcal{W}_C(k)) \quad (102)$$

where  $S_0(k) = 2\pi^2 k^2 I/\beta$  is the classical action for a free rotor making  $k$  complete circuits in a given time interval. It contains a dynamical contribution, proportional to the classical action, that is modulated by a purely topological term, the Wilson loop integral  $\mathcal{W}_C(k)$ . At higher temperatures  $z$  is largely dominated by contributions from the classical action and so we investigate the behavior of  $\mathcal{Z}$  in the low temperature  $\beta \rightarrow \infty$  limit. A detailed derivation is given in Appendix B and according to Eqs. (B12)

$$z \rightarrow 2 \sqrt{\frac{2\pi I}{\beta}} \exp(\beta V(\theta)) \times \sum_k \exp(-S_0(k)) \cos(2\pi k \Omega) \quad (103)$$

in that limit.  $S_0(k)$  is the Wick rotated action for a free rotor undergoing  $k$  circuits and

$$V(\theta) = -\frac{\cos^2 \theta}{I} + \alpha_0 + \frac{I \alpha_1^2}{2} \\ \Omega = -\frac{\sin^2 \theta}{4} + \sqrt{\frac{\sin^2 \theta}{16} + \cos^2 \theta}. \quad (104)$$

In Fig. (9) we plot

$$-\frac{\partial \ln z}{\partial \beta}$$

as  $\beta \rightarrow \infty$ , and which represent the ground state energy. The solid line denotes the ground state energy for Hamiltonian (87), the dashed line the adiabatic energy  $e_g$ , and the circle icons denote energies obtained in the PSS approximation and calculated using expression (103) for the partition function. The latter approximation is accurate for values  $\Delta/e_g \gg 1$ . According to expression (103), the term  $m\Omega$  is independent of the temperature parameter  $\beta$  and is therefore of topological origin. The cross icons in that figure represent the energies obtained by artificially setting  $\Omega = 0$  in expression (103). The difference between those values and the ones laying on the solid line, underscores the significance of that topological contribution. Interestingly, unlike in the high temperature limit, the value for  $2\pi m\Omega$  does not equal the Wilson loop integral  $\mathcal{W}_C$  of the projected gauge potential  $\mathbf{A}'_p$ .

## VII. SUMMARY AND DISCUSSION

The gauge principle forms a cornerstone to our modern understanding of the fundamental constituents of matter.

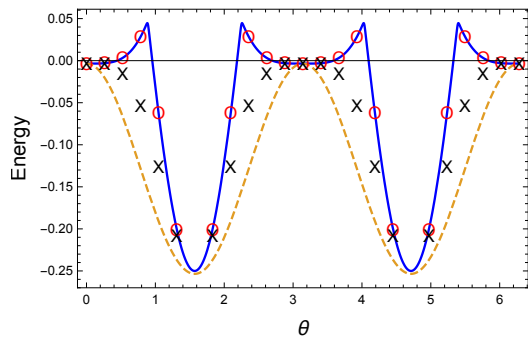


FIG. 9: Ground state energy of Hamiltonian (87) as a function of gauge parameter  $\theta$ .

Quantum Electrodynamics (QED) is the best known example of an Abelian gauge theory, and its non-Abelian generalization illuminates the landscape within the nucleus.

Gauge invariance guarantees charge conservation, and is the guiding principle that insures a gauge field's raison'detre. For example, the following Hamiltonian (up to a surface term) for a scalar field  $\phi$

$$\mathcal{H} = \frac{-1}{2m} \int d^3\mathbf{x} \phi^\dagger(\mathbf{x}) \nabla^2 \phi(\mathbf{x}) \quad (105)$$

is not invariant under the replacement of field operator  $\phi(\mathbf{x})$  with  $\exp(i\Lambda(\mathbf{x}))\phi(\mathbf{x})$ . Introducing an auxiliary quantum field  $\mathbf{A}$  so that

$$\mathcal{H} = \frac{-1}{2m} \int d^3\mathbf{x} \phi^\dagger(\mathbf{x}) (\nabla - i\mathbf{A})^2 \phi(\mathbf{x}) \quad (106)$$

gauge invariance is enforced provided that as  $\phi(\mathbf{x}) \rightarrow \exp(i\Lambda(\mathbf{x}))\phi(\mathbf{x})$ ,  $\mathbf{A} \rightarrow \mathbf{A} + \nabla\Lambda$ .

In quantum mechanics (QM) the Schrödinger equation is not invariant under a gauge transformation of the wave amplitude, however the eigenvalues of operators, i.e. observables, are. Dirac[33] argued that a Schrödinger description in which the wave function is minimally coupled to a gauge potential is equivalent to a gauge field free theory whose wave amplitudes posses non-integrable[11, 33], or Peirls[34] phase factors.

In this paper we provided examples of pedestrian quantum systems in which gauge structures arise in a natural manner without the need to summon the former. This feature of QM has long been noted in studies of atomic and molecular systems[15–17, 22]. But, as those descriptions require the application of Born-Oppenheimer like approximations, predictions are open to interpretations that attracts skepticism[35]. For example, laboratory searches for the Molecular Aharonov-Bohm Effect (MAB)[36], in the reactive scattering of molecules, has had a long and controversial history[37–39]. In this paper we addressed some of those concerns in two ways, (i) we identified systems that allow analytic solutions, and (ii) explicitly demonstrated the dependence of gauge invariant quantities (e.g. the partition function) on the

Wilson loop integral of a non-trivial gauge potential. Furthermore, our analysis did not require the semi-classical notion of adiabaticity, or degeneracy in the adiabatic eigenvalues. Unlike gauge quantum fields, quantum mechanical gauge potentials, discussed here, do not exhibit dynamic content (but see Appendix C).

In the remaining discussion we address possible laboratory demonstrations of effects predicted and discussed in this paper. Though we are unable to comment on the viability of present day laboratory capabilities to realize the double slit system discussed in the introduction, we anchor our focus on recent laboratory efforts to simulate a coherent quantum rotor. For example, a planar quantum rotor was simulated[40] in a cylindrical symmetric ion trap in which a pair of  $^{40}\text{Ca}^+$  ions formed a two-ion Coulomb crystal. That experiment demonstrated a capability to prepare and control angular momentum states. Along those lines we propose trapping a spin - 1/2 ion in a toroidal trap as shown in Fig (10). In that figure a positively charged spin-1/2 ion, such as  $\text{Ca}^+$  in its ground state, is trapped in the torus. Instead, one can also consider a pair ions forming a Coulomb crystal, as described in [40]. The latter simulates, after factoring out the center of mass motions, a single ion rotor. However, for the sake of illustration, we limit this discussion to a toroidal trap configuration. We thread an electric current along

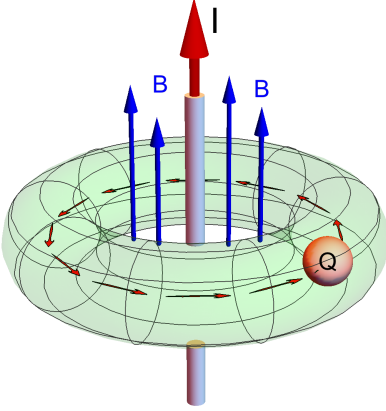


FIG. 10: Illustration of a toroidal trap in which an ion of charge  $Q$  simulates the motion of a planar, quasi-rigid, rotor. A current  $I$  (red arrow) threading the doughnut hole induces an axial magnetic field. The system is subjected to a background magnetic bias field (blue) arrow.

the symmetry axis piercing the doughnut hole to induce a magnetic field along the axial direction of the torus. Alternatively, an axial magnetic field can also be gen-

erated by joining a solenoid at its ends to form a torus (i.e. a micro-tokamak). In addition to the toroidal axial field, generated by current  $I$ , a constant homogeneous bias magnetic field of magnitude  $B_0$  parallel the symmetry axis is applied. The Hamiltonian for this system is

$$H = \frac{-\hbar^2}{2m} (\nabla \mathbb{1} - i \frac{q}{\hbar c} \mathbf{A}_0)^2 + \mathbf{U}(\phi) \Delta(\rho) \mathbf{U}^\dagger(\phi) + V_{trap} \quad (107)$$

where, in a cylindrical coordinate system,

$$\mathbf{A}_0 = \left( \hat{\phi} \frac{B_0 \rho}{2} + \hat{z} \frac{\mu_0 I}{2\pi} \ln \rho \right) \mathbb{1} \quad (108)$$

is the Landau gauge vector potential for the total magnetic field.  $\mathbf{U}(\phi)$  is given by Eq. (22),

$$\cos \theta = \frac{B_0}{\sqrt{B_0^2 + \left(\frac{\mu_0 I}{2\pi \rho}\right)^2}},$$

$q$  is the charge of the ion,  $\mu_0$  the magnetic constant,

$$\Delta(\rho) = \mu \sqrt{B_0^2 + \left(\frac{I \mu_0}{2\pi \rho}\right)^2} \sigma_3,$$

and  $V_{trap}$  is a trapping potential.

In the adiabatic representation, and assuming that  $V_{trap}$  is independent of spin, we obtain the eigenvalue Schrödinger equation,

$$\begin{aligned} & \frac{-\hbar^2}{2m} (\nabla - i\mathcal{A})^2 F(\mathbf{r}) + \Delta(\rho) F(\mathbf{r}) + \\ & V_{trap}(\mathbf{r}) F(\mathbf{r}) = E F(\mathbf{r}) \end{aligned} \quad (109)$$

where

$$\begin{aligned} \mathcal{A} &= i\mathbf{U}^\dagger \nabla \mathbf{U} + \mathbf{A}_0 = \\ & \frac{\hat{\phi}}{2\rho} \begin{pmatrix} \cos \theta - 1 + \frac{q}{\hbar c} B_0 \rho^2 & i \sin \theta \exp(-i\phi) \\ -i \sin \theta \exp(i\phi) & (1 - \cos \theta) + \frac{q}{\hbar c} B_0 \rho^2 \end{pmatrix} + \\ & \hat{\rho} \begin{pmatrix} 0 & -\frac{1}{2} \exp(-i\phi) \theta'(\rho) \\ -\frac{1}{2} \exp(i\phi) \theta'(\rho) & 0 \end{pmatrix} \\ & - \hat{z} \frac{q \mu_0 I}{2 \hbar c \pi} \ln \rho \begin{pmatrix} 1 & 0 \\ 0 & 1 \end{pmatrix}. \end{aligned} \quad (110)$$

Assuming that the trap potential is effective in freezing the degrees of freedom in the radial and  $\hat{z}$  direction, and for a large Zeeman energy gap  $\Delta$ , we replace the 3D Schrödinger Eq. (109) with an effective 1D equation corresponding to a rigid planar rotor,

$$\begin{aligned} & \frac{-\hbar^2}{2m\rho_0^2} (\partial_\phi - i\mathcal{A}_{eff})^2 F(\phi) + \Delta(\rho_0) F(\phi) = E F(\phi) \\ & \mathcal{A}_{eff} = \\ & \frac{1}{2} \begin{pmatrix} \cos \theta(\rho_0) - 1 + \frac{q\Phi}{\hbar\pi c} & 0 \\ 0 & 1 - \cos \theta(\rho_0) + \frac{q\Phi}{\hbar\pi c} \end{pmatrix} \end{aligned} \quad (111)$$

where  $\rho_0$  is the equilibrium value of the radial coordinate, and  $\Phi = B_0\pi\rho_0^2$  is the total magnetic flux enclosed by the rotor. By tuning the current  $I$  and the bias field  $B_0$  we can alter and discriminate the values of the Wilson loop for different spin states. For example, if

$$\cos\theta(\rho_0) - 1 + \frac{q\Phi}{\hbar\pi c} = 0$$

then,

$$\mathcal{A}_{eff} \rightarrow \begin{pmatrix} 0 & 0 \\ 0 & \frac{q\Phi}{\hbar\pi c} \end{pmatrix}. \quad (112)$$

In this scenario the upper Zeeman level undergoes the motion of a free rotor, whereas the lower component experience an effective AB flux tube with charge  $\Phi$ . Such a capability, if realized, could find application as a novel magnetometer and rotational sensor.

The planar rotor has also been used as a model for the anyon[7]. In adiabatic transport about a flux tube it can acquire a non-integer phase (modulus  $2\pi$ ) as it completes one circuit. In the rotor systems discussed here adiabatic transport is problematic as an initial wave packet spreads in time. However, as a closed system, it eventually revives to its original shape. For example, the propagator for a spin-1/2 planar rotor coupled to a Wu-Yang flux tube of ‘‘charge’’  $\alpha$  is given by

$$G(\phi t; \phi' t' = 0) = \sum_m \frac{1}{2\pi} \exp(im(\phi - \phi')) \exp(-i\frac{\hbar^2}{2I}(m - \alpha\sigma_3)^2 t)$$

Or,

$$\exp(-i\frac{\hbar^2\alpha^2 t}{2I}) \sum_m \frac{1}{2\pi} \exp(im(\phi - \phi' + \sigma_3 \frac{\hbar^2 t \alpha}{I})) \times \exp(-i\frac{\hbar^2 m^2 t}{2I}). \quad (113)$$

Now at the revival[41] time  $t_N = \frac{4\pi I N}{\hbar^2}$ , where  $N$  is an integer,

$$G(\phi t_N; \phi') = \frac{1}{2\pi} \exp(i\Delta\phi_N \frac{\alpha}{2}) \sum_m \exp(im(\phi - \phi' + \sigma_3 \Delta\phi_N)) = \exp(i\Delta\phi_N \frac{\alpha}{2}) \begin{pmatrix} \delta(\phi - \phi' + \Delta\phi_N) & 0 \\ 0 & \delta(\phi - \phi' - \Delta\phi_N) \end{pmatrix} \quad (114)$$

where  $\Delta\phi_N = t_N \frac{\hbar^2\alpha}{I} = 4\pi N\alpha$ . Thus an arbitrary initial, localized, wave packet is displaced, depending on its spin state, by an amount  $\pm\Delta\phi_N$ . Suppose  $\alpha = m/p$  is a rational number where  $p$  is even, then the packet returns to its original starting point, i.e.  $\Delta\phi = 0 \text{ Mod } 2\pi$  at  $t_{N^*}$  for  $N^* = p/2$ . So if a localized packet at  $t = 0$  has the form

$$\psi(\phi, t = 0) = \begin{pmatrix} \psi_u(\phi) \\ \psi_d(\phi) \end{pmatrix}, \quad (115)$$

it evolves to

$$\psi(\phi, t_{N^*}) = \begin{pmatrix} \exp(iW_m(\alpha))\psi_u(\phi) \\ \exp(-iW_m(\alpha))\psi_d(\phi) \end{pmatrix} \quad (116)$$

where

$$W_m(\alpha) \equiv \oint_m d\mathbf{R} \cdot \mathbf{A}_{AB} \\ \mathbf{A}_{AB} = \hat{\phi} \frac{\alpha}{R} \quad (117)$$

is the argument of a Wilson loop integral with winding number  $m$ . A similar argument can be used when  $p$  is odd. Expression (116) demonstrates that an arbitrary wave packet revives, up to a topological phase factor  $\exp(iW_m \alpha \sigma_3)$ , at its initial position.

On a final note, at the time of writing I have become aware of recent literature in which similar themes, presented in this paper, are discussed. Synthetic gauge structures on a ring lattice have been explored in [42], and non-Abelian Wu-Yang structures have been observed in optical systems[43, 44]

## ACKNOWLEDGMENTS

I wish to acknowledge support by the National Supercomputing Institute for use of the Intel Cherry-Creek computing cluster. Part of this work was also made possible by support from a NSF-QLCI-CG grant 1936848.

## Appendix A

According to Eqs. (69) and (71) the Schrödinger equation for a rotor with unit radius is

$$-\frac{1}{2I} \left( \frac{\partial}{\partial\phi} - i\mathbf{a} \right)^2 F + \mathbf{\Delta} F = i \frac{\partial F}{\partial t} \quad (A1)$$

where the gauge potential

$$\mathbf{a} = q \begin{pmatrix} \cos\theta & \exp(i\gamma)\sin\theta \\ \exp(-i\gamma)\sin\theta & -\cos\theta \end{pmatrix}, \quad (A2)$$

where  $q$  is an integer and  $\theta, \gamma$  are parameters. To solve for its energy spectrum we let  $F = \frac{\exp(im\phi)}{\sqrt{2\pi}} \mathbf{c}$  so that

$$\frac{(m\mathbf{1} - \mathbf{a})^2}{2I} \mathbf{c} + \mathbf{\Delta} \mathbf{c} = i\dot{\mathbf{c}} \quad (A3)$$

or  $\mathbf{h} \mathbf{c} = i\dot{\mathbf{c}}$

$$\mathbf{h} = \mathbf{1} \frac{(m^2 + q^2)}{2I} - \frac{m}{I} \begin{pmatrix} \cos\theta - \frac{I}{m}\Delta & \exp(i\gamma)\sin\theta \\ \exp(-i\gamma)\sin\theta & -\cos\theta + \frac{I}{m}\Delta \end{pmatrix} \quad (A4)$$

where we used the fact that  $\mathbf{a} \cdot \mathbf{a} = q^2 \mathbf{1}$ . The eigenvalues of  $\mathbf{h}$  are

$$e(m) = e_0(m) \pm e_1(m) \\ e_0(m) = \frac{m^2 + q^2}{2I} \\ e_1 = \frac{\sqrt{m^2 q^2 + I^2 \Delta^2 - 2I m q \Delta \cos\theta}}{2I} \quad (A5)$$



and, the partition function,

$$\mathcal{Z} = 2 \sum_m \exp(-\beta e_0(m)) \cosh(\beta e_1(m)) \quad (\text{A6})$$

where  $\beta$  is the inverse temperature. Consider the limit  $\Delta \ll 1$ , in which

$$\mathcal{Z} \rightarrow 2 \sum_m \exp(-\beta \frac{m^2 + 1}{2I}) \times \cosh(\beta(\frac{m}{I} - \Delta \cos \theta)). \quad (\text{A7})$$

Taking the Poisson transform of the r.h.s of Eq. (A7), we find

$$\mathcal{Z} \rightarrow 2 \sqrt{\frac{2\pi I}{\beta}} \sum_m \exp(-\frac{2I\pi^2 m^2}{\beta}) \cosh(\beta \Delta \cos \theta). \quad (\text{A8})$$

Thus, in this limit the partition function assumes the form of a free rotor in the presence of a constant ‘‘scalar’’ potential  $\Delta \cos \theta$ .

In the other extreme,  $I \Delta \gg 1$ ,

$$\mathcal{Z} \rightarrow 2 \sum_m \exp(-\beta \frac{m^2 + 1}{2I}) \times \cosh(\beta(\Delta - \frac{m}{I} \cos \theta)) \quad (\text{A9})$$

or, applying the Poisson summation formula,

$$\mathcal{Z} \rightarrow 2 \sqrt{\frac{2\pi I}{\beta}} \cosh(\beta \Delta) \exp(-\beta \frac{\sin^2 \theta}{2I}) \times \sum_m \exp(-\frac{2\pi^2 m^2 I}{\beta}) \cos(2\pi m \cos \theta). \quad (\text{A10})$$

In Fig. (11) we plotted the logarithm of the ratio  $\mathcal{Z}/\mathcal{Z}_0$  where

$$\mathcal{Z}_0 \equiv 2 \sqrt{\frac{2\pi I}{\beta}} \cosh(\beta \Delta) \exp(-\beta \frac{\sin^2 \theta}{2I}).$$

In that figure the solid lines are calculated using the exact values Eq. (A6) for  $\mathcal{Z}$ , whereas the dashed lines represent the value obtained using the approximate expression (A10). According to Eq. (A10), the ratio

$$\mathcal{Z}/\mathcal{Z}_0 = \sum_m \exp(-\frac{2\pi^2 m^2 I}{\beta}) \cos(2\pi m \cos \theta)$$

in the limit  $\beta \gg 1$ . The variation of this ratio, shown in Fig. (11), demonstrates the role of the topological contribution  $\cos(2\pi m \cos \theta)$  to the, gauge invariant, partition function.

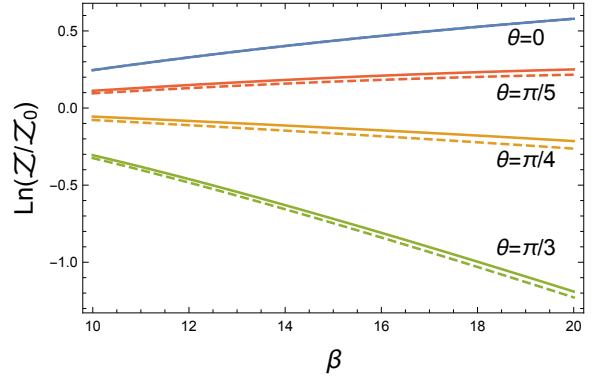


FIG. 11: Plot of ratio  $\text{Ln}(\mathcal{Z}/\mathcal{Z}_0)$  as a function of the inverse temperature  $\beta$ . The values  $I = 1$ ,  $\Delta = 100$ , were used to obtain this data.

## Appendix B

According to Eq. (98) the reduced partition function

$$z = 2 \sum_m \exp(-\beta e_0) \cosh(\beta e_1) \\ e_0 = \frac{m^2 + \cos^2 \theta}{2I} \\ e_1 = \sqrt{\Delta^2 + \frac{m^2}{I^2} \cos^2 \theta}. \quad (\text{B1})$$

At cold temperatures as, i.e.  $\beta \rightarrow \infty$ , the approximation

$$e_1 \approx \alpha_0 + \alpha_1 |m| \\ \alpha_0 = \Delta \\ \alpha_1 = -\Delta + \sqrt{\Delta^2 + \frac{\cos^2 \theta}{I^2}} \quad (\text{B2})$$

is appropriate. Therefore, we need to evaluate

$$z = 2 \sum_m \exp(-\beta(\frac{m^2 + \cos^2 \theta}{2I})) \times \cosh(\beta(\alpha_0 + |m|\alpha_1)) \quad (\text{B3})$$

or

$$z = 2 \exp(-\beta \frac{\cos^2 \theta}{2I}) \sum \exp(-\beta \frac{m^2}{2I}) \times \left( \cosh(\beta \alpha_0) \cosh(\beta \alpha_1 |m|) + \sinh(\beta \alpha_0) \sinh(\beta \alpha_1 |m|) \right). \quad (\text{B4})$$

The Poisson transform of Eq. (B4) leads to

$$z = 2 \exp(-\frac{\beta \cos^2 \theta}{2I}) \sqrt{\frac{2\pi I}{\beta}} \left( \cosh(\alpha_0 \beta) \times \sum_k \exp(-\frac{2\pi^2 I k^2}{\beta}) \exp(\frac{\alpha_1^2 I \beta}{2}) \cos(2\pi I k \alpha_1) - \frac{2}{\sqrt{\pi}} \sinh(\alpha_0 \beta) \sum_k \text{Im} D_F(\sqrt{\frac{I}{2\beta}}(2\pi k - i \alpha_1 \beta)) \right) \quad (\text{B5})$$

where  $D_F$  is the Dawson integral[45] and where the summation is over all integers  $k$ . It is useful to express the latter in terms of a confluent hypergeometric function [45]

$$D_F(\xi) = \xi \exp(-\xi^2) {}_1F_1\left(\frac{1}{2}, \frac{3}{2}, \xi^2\right). \quad (\text{B6})$$

For  $|\xi| \gg 1$  we use the asymptotic expansion for the Kummer function[46]

$${}_1F_1\left(\frac{1}{2}, \frac{3}{2}, \xi^2\right) \rightarrow \frac{\exp(\xi^2)}{2\xi^2} \pm \frac{i\sqrt{\pi}}{2\sqrt{\xi^2}} \quad (\text{B7})$$

where the  $\pm$  sign refers to the cases

$$-\frac{\pi}{2} < \arg(\xi^2) < \frac{3\pi}{2} \quad \& \quad -\frac{3\pi}{2} < \arg(\xi^2) \leq -\frac{\pi}{2}$$

respectively. Or

$$D_F(\xi) \rightarrow \frac{1}{2\xi} \pm \frac{i\sqrt{\pi}}{2} \exp(-\xi^2) \quad (\text{B8})$$

where  $\pm$  corresponds to  $\text{Re}(\xi) > -\text{Im}(\xi)$  and  $\text{Re}(\xi) < -\text{Im}(\xi)$  respectively. Since  $\xi = \sqrt{\frac{I}{2\beta}}(2\pi k - i\beta\alpha_1)$  we find that as  $\beta \rightarrow \infty$  ( $\alpha_1 \neq 0$ )

$$\begin{aligned} \text{Im } D_F\left(\sqrt{\frac{I}{2\beta}}(2\pi k - i\alpha_1\beta)\right) \rightarrow \\ \sqrt{\frac{\beta}{2I}} \frac{\beta\alpha_1}{4\pi^2 k^2 + \alpha_1^2 \beta^2} \pm \\ \frac{\sqrt{\pi}}{2} \exp\left(\frac{\alpha_1^2 I \beta}{2}\right) \exp\left(-\frac{2\pi^2 I k^2}{\beta}\right) \cos(2\pi I k \alpha_1) \end{aligned} \quad (\text{B9})$$

Thus, if  $\alpha_0 > 0$ ,

$$\begin{aligned} z \approx \sqrt{\frac{2\pi I}{\beta}} \exp\left(-\frac{\beta \cos^2 \theta}{2I}\right) \exp(\alpha_0 \beta) \exp\left(\frac{\alpha_1^2 I \beta}{2}\right) \times \\ \sum_k \exp\left(-\frac{2\pi^2 I k^2}{\beta}\right) \cos(2\pi I \alpha_1 k) g(k) \end{aligned} \quad (\text{B10})$$

where

$$\begin{aligned} g(k) &= 2 \quad \text{for } 2\pi k < \alpha_1 \beta \\ g(k) &= 0 \quad \text{for } 2\pi k > \alpha_1 \beta \end{aligned}$$

and we used the fact

$$\sum_k \frac{\alpha_1 \beta}{4\pi^2 k^2 + \alpha_1^2 \beta^2} = \frac{1}{2} \coth \frac{\alpha_1 \beta}{2} \approx \frac{1}{2} \quad (\text{B11})$$

in this limit. Using definitions (B2) and so

$$\alpha_0 = \frac{\sin^2 \theta}{4I} \quad \alpha_1 = -\frac{\sin^2 \theta}{4I} + \frac{\sqrt{\frac{\sin^2 \theta}{16} + \cos^2 \theta}}{I},$$

and  $\Delta = \frac{\sin^2 \theta}{4I}$  we find that,

$$\begin{aligned} z \rightarrow 2\sqrt{\frac{2\pi I}{\beta}} \exp(\beta V(\theta)) \times \\ \sum_k \exp(-S_0(k)) \cos(2\pi k \Omega) \end{aligned} \quad (\text{B12})$$

where  $S_0(k)$  is the Wick rotated action for a free rotor undergoing  $k$  circuits and

$$\begin{aligned} V(\theta) &= -\frac{\cos^2 \theta}{I} + \alpha_0 + \frac{I\alpha_1^2}{2} \\ \Omega &= -\frac{\sin^2 \theta}{4} + \sqrt{\frac{\sin^2 \theta}{16} + \cos^2 \theta}. \end{aligned} \quad (\text{B13})$$

### Appendix C

We first demonstrate that a particle in the presence of a quantized gauge field begets a multicomponent wave equation whose amplitudes are coupled to a non-Abelian gauge potential. As an example, consider the Hamiltonian for a charged (first quantized) particle coupled to a quantized, transverse, Maxwell gauge field,

$$\begin{aligned} H &= \frac{1}{2m} (\mathbf{p} - \mathbf{A}_r)^2 + \sum_{k\lambda} \hbar\omega_{k\lambda} a_{\mathbf{k}\lambda}^\dagger a_{\mathbf{k}\lambda} \\ \mathbf{A}_r &= \sum_{k\lambda} \left( \mathbf{A}_{\mathbf{k}\lambda}^* a_{\mathbf{k}\lambda} + \mathbf{A}_{\mathbf{k}\lambda} a_{\mathbf{k}\lambda}^\dagger \right) \end{aligned} \quad (\text{C1})$$

Here  $\mathbf{p}$  is the particle momentum operator conjugate to  $\mathbf{r}$ .  $a_{\mathbf{k}\lambda}$ ,  $a_{\mathbf{k}\lambda}^\dagger$  are, respectively, photon destruction and creation operators that satisfy commutation relations  $[a_{\mathbf{k}\lambda}, a_{\mathbf{k}'\lambda'}^\dagger] = \delta_{\mathbf{k},\mathbf{k}'} \delta_{\lambda,\lambda'}$ , and  $\mathbf{A}_{\mathbf{k}\lambda}^*$  is an amplitude for a photon with momentum  $\mathbf{k}$ , and polarization  $\lambda$ . For the sake of simplicity, and without loss of generality, we consider only single mode field quanta that are eigenstates of the number operator  $a^\dagger a$ , where we suppressed the mode index. The eigenstates of the radiation field

$$H_{rad} \equiv \hbar\omega a^\dagger a$$

are labeled by the occupation number and so an eigenstate of Hamiltonian (C1), can always be written as a linear combination

$$\Psi = \sum_n f_n(\mathbf{r}) |n\rangle \quad (\text{C2})$$

where  $|n\rangle$  is an eigenstate of the number operator  $a^\dagger a$  and  $n$  is the occupation number. Using expression (C2) and treating the amplitudes  $f_n(\mathbf{r})$  as variational parameters we arrive, using the fact that the set  $|n\rangle$  are orthonormal, the set of coupled equations,

$$\frac{1}{2m} (\nabla - i\mathbf{A}_r)^2 \underline{F}(\mathbf{r}) + \underline{V} \underline{F}(\mathbf{r}) = E \underline{F}(\mathbf{r}). \quad (\text{C3})$$

Here

$$\underline{F}(\mathbf{r}) \equiv \begin{pmatrix} f_1(\mathbf{r}) \\ f_2(\mathbf{r}) \\ \vdots \end{pmatrix} \quad (\text{C4})$$

is an infinite dimensional column matrix.  $\underline{\mathbf{A}}_r$  is a square matrix whose  $nm$ th entry  $\mathbf{A}_{nm} = \langle n | \mathbf{A}_r | m \rangle$ , and  $\underline{V}$  is a diagonal matrix whose  $n$ th entry is  $n \hbar \omega$ .

Consider a Hilbert space generated by bosonic operators  $a, a^\dagger$  so that  $[a, a^\dagger] = 1$ . This space is spanned by the basis vectors

$$|n\rangle = \frac{(a^\dagger)^n}{\sqrt{n!}} |0\rangle \quad (\text{C5})$$

where  $a|0\rangle = 0$ . In this space we define a Hamiltonian

$$H_{BO} = e(a^\dagger a) \quad (\text{C6})$$

where  $e$  is an arbitrary function. The spectrum of  $H_{BO}$  is  $e(n)$  for  $n \in \mathbb{Z} \geq 0$ .

We now posit the Hamiltonian

$$H = \frac{\mathbf{p}^2}{2m} + U H_{BO} U^\dagger, \quad (\text{C7})$$

which is a straight-forward generalization of the finite dimensional models discussed in the main section. Here,  $U$  is a unitary operator that, in general, is a function of  $\mathbf{r}$  and  $a, a^\dagger$ .

For example, let

$$U = \exp(-i\phi a^\dagger a) \exp(-i\lambda(a + a^\dagger)) \exp(i\phi a^\dagger a) \quad (\text{C8})$$

where  $\phi$  is the azimuthal angle in a cylindrical coordinates system, and  $\lambda$  is a real valued parameter. Because the eigenvalues of the number operator  $a^\dagger a$  are integers,  $U$  is single valued, i.e.  $U(\phi = 0) = U(\phi = 2\pi)$ , and so we can express the system amplitude

$$\Psi = \sum_n f_n(\mathbf{r}) U |n\rangle. \quad (\text{C9})$$

Using this ansatz we arrive at the set of equations (C3) where now the amplitudes  $f_n(\mathbf{r})$  are coupled to

$$\begin{aligned} \underline{V}_{nm} &= \langle n | H_{BO} | m \rangle = e(n) \delta_{nm} \\ \underline{\mathbf{A}}_{nm} &= \langle n | \mathbf{A} | m \rangle \\ \mathbf{A} &= \frac{i\hat{\phi}}{r} U^\dagger \partial_\phi U = \frac{i\hat{\phi}}{r} \left( -iU^\dagger a^\dagger a U + i a^\dagger a \right) = \\ &\hat{\phi} \frac{i\lambda}{r} \left( a \exp(i\phi) - a^\dagger \exp(-i\phi) \right) + \hat{\phi} \frac{\lambda^2}{r}. \end{aligned} \quad (\text{C10})$$

Here  $\mathbf{A}$  describes a pure gauge. Alternatively, we could induce a unitary transformation

$$\begin{aligned} H' &= U^\dagger H U = U^\dagger \frac{\mathbf{p}^2}{2m} U + H_{BO} = \\ &\frac{1}{2m} (\mathbf{p} - \mathbf{A})^2 + e(a^\dagger a) \end{aligned} \quad (\text{C11})$$

so that  $H'$  describes a particle minimally coupled to a dynamical Abelian gauge field  $\mathbf{A}$ . In this picture the ansatz  $\sum_n f'_n(\mathbf{r}) |n\rangle$  leads to identical equations for the amplitudes  $f'_n(\mathbf{r})$  described above.

Although  $\mathbf{A}$  is a pure gauge, low energy eigensolutions to  $H'$  exhibit, as we demonstrate below, non-trivial effective gauge structure. For example, suppose that  $e(n) \gg e(0)$  for  $n > 0$ . We can then employ the PSS approximation, which begets the Schrödinger equation

$$\frac{1}{2m} (\nabla - i\mathbf{A}_{eff})^2 F(\mathbf{r}) + \underline{V}_{eff} F(\mathbf{r}) = E F(\mathbf{r}) \quad (\text{C12})$$

for the ground state scalar amplitude  $F(\mathbf{r})$ . Here

$$\mathbf{A}_{eff} = \hat{\phi} \frac{\lambda^2}{r} \quad (\text{C13})$$

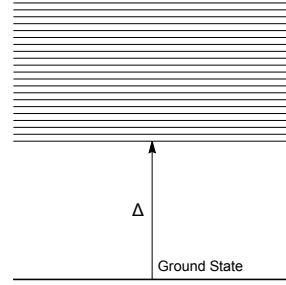


FIG. 12

is the gauge potential of an Aharonov-Bohm flux tube of charge  $\lambda^2$ , and

$$\underline{V}_{eff} = e_0 + \frac{1}{2m} \sum_{n \neq 0} \mathbf{A}_{0n} \cdot \mathbf{A}_{n0}. \quad (\text{C14})$$

is an effective scalar potential that is the sum of the adiabatic ground state energy  $e_0 \equiv e(0) = \langle 0 | e(a^\dagger a) | 0 \rangle$  and the correction

$$\begin{aligned} &\frac{1}{2m} \sum_{n \neq 0} \mathbf{A}_{0n} \cdot \mathbf{A}_{n0} = \\ &\frac{\lambda^2}{2mr^2} \langle 0 | a \exp(i\phi) | 1 \rangle \langle 1 | \exp(-i\phi) a^\dagger | 0 \rangle = \\ &\frac{1}{2m} \frac{\lambda^2}{r^2}. \end{aligned} \quad (\text{C15})$$

We can think of the latter as a self-energy induced by the emission and re-adsorption of gauge quanta, thus demonstrating dynamical content encapsulated in  $\mathbf{A}$ .

- 
- [1] A. Aharonov and D. Bohm, *Phys. Rev.* **115**, 485 (1959).
- [2] P. Ball, *Beyond Weird* (University of Chicago Press, 2018).
- [3] R. Feynman, R. Leighton, and M. Sands, *The Feynman Lectures on Physics, Vol. III: The New Millennium Edition: Quantum Mechanics*, The Feynman Lectures on Physics (Basic Books, 2011).
- [4] A. Peruzzo, P. Shadbolt, N. Brunner, S. Popescu, and J. L. O'Brien, *Science* **338**, 634 (2012).
- [5] Y.-H. Kim, R. Yu, S. P. Kulik, Y. Shih, and M. O. Scully, *Phys. Rev. Lett.* **84**, 1 (2000).
- [6] D. J. Thouless, M. Kohmoto, M. P. Nightingale, and M. den Nijs, *Phys. Rev. Lett.* **49**, 405 (1982).
- [7] F. Wilczek, *Physical Review Letters* **49**, 957 (1982).
- [8] M. Z. Hasan and C. L. Kane, *Rev. Mod. Phys.* **82**, 3045 (2010).
- [9] D. S. Sankar, M. Freedman, and C. Nayak, *Physics Today* **59** (2006).
- [10] J. Preskill, (1997), arXiv:quant-ph/9712048.
- [11] T. T. Wu and C. N. Yang, *Phys. Rev. D* **12**, 3845 (1975).
- [12] P. A. Horváthy, *Phys. Rev. D.* **33**, 407 (1986).
- [13] J. March-Russell, J. Preskill, and F. Wilczek, *Phys. Rev. Lett.* **68**, 2567 (1992).
- [14] Y. Mankeenko, (2009), arXiv:0906.4487v1.
- [15] C. A. Mead and G. D. Truhlar, *The Journal of Chemical Physics* **70**, 2284 (1979).
- [16] J. Moody, A. Shapere, and F. Wilczek, *Phys. Rev. Lett.* **56**, 893 (1986).
- [17] B. Zygelman, *Phys. Lett. A* **125**, 476 (1987).
- [18] R. Jackiw, *Comments At. Mol. Phys.* **21** (1988).
- [19] B. Zygelman, *Physical Review Letters* **64**, 256 (1990).
- [20] B. Zygelman, *Phys. Rev. A.* **92**, 043620 (2015).
- [21] F. Wilczek and A. Zee, *Phys. Rev. Lett.* **52**, 2111 (1984).
- [22] B. Zygelman and A. Dalgarno, *Phys. Rev. A* **33**, 3853 (1986).
- [23] M. V. Berry, in *Geometric Phases in Physics*, edited by A. Shapere and F. Wilczek (World Scientific Publishing Company, 1989) p. 1.
- [24] The Wilson loop integral for a WY flux tube is twice that of a single AB flux tube.
- [25] P. Dirac, *Lectures on Quantum Mechanics*, Belfer Graduate School of Science, monograph series (Dover Publications, 2001).
- [26] A. Scardicchio, *Physics Letters A* **200**, 7 (2002).
- [27] R. Bellman, *A Brief Introduction to Theta Functions* (Dover Publications, 2013).
- [28] L. Schulman, *Techniques and Applications of Path Integration* (Dover Publications, 2005).
- [29] M. V. Berry, *Proc. R. Soc. Lond. A* **392**, 45 (1984).
- [30] E. Cohen, H. Larocque, F. Bouchard, F. Nejdattari, Y. Gefen, and E. Karimi, *Nature Reviews Physics* **1**, 437 (2019).
- [31] Born M. and K. Huang, *Dynamical Theory of Crystal Lattices* (Oxford University Press, 1954).
- [32] N. F. Mott and H. S. W. Massey, *The Theory of Atomic Collisions*, 2nd ed. (Oxford, 1949) p. 128.
- [33] P. A. M. Dirac, *Royal Society of London Proceedings Series A* **133**, 60 (1931).
- [34] K. Jiménez-García, L. J. LeBlanc, R. A. Williams, M. C. Beeler, A. R. Perry, and I. B. Spielman, *Phys. Rev. Lett.* **108**, 225303 (2012).
- [35] S. K. Min, A. Abedi, K. S. Kim, and E. K. U. Gross, *Phys. Rev. Lett.* **113**, 263004 (2014).
- [36] C. A. Mead, *Chemical Physics* **49**, 23 (1980).
- [37] B. Zygelman, *Journal of Physics B: Atomic, Molecular and Optical Physics* **50**, 025102 (2016).
- [38] B. K. Kendrick, *The Journal of Chemical Physics* **148**, 044116 (2018).
- [39] D. Yuan, Y. Guan, W. Chen, H. Zhao, S. Yu, C. Luo, Y. Tan, T. Xie, X. Wang, Z. Sun, D. H. Zhang, and X. Yang, *Science* **362**, 1289 (2018).
- [40] E. Urban, N. Glikin, S. Mouradian, K. Krimmel, B. Hemmerling, and H. Haefner, *Phys. Rev. Lett.* **123**, 133202 (2019).
- [41] R. Robinett, *Physics Reports* **392**, 1 (2004).
- [42] K. K. Das and M. Gajdacz, *Scientific Reports* **9**, 14220 (2019).
- [43] Y. Yang, C. Peng, D. Zhu, H. Buljan, J. D. Joannopoulos, B. Zhen, and M. Soljačić, *Science* **365**, 1021 (2019).
- [44] Y. Chen, R.-Y. Zhang, Z. Xiong, Z. H. Hang, J. Li, J. Q. Shen, and C. T. Chan, *Nature Communications* **10**, 3125 (2019).
- [45] V. Nijimbire, (2017), arXiv:1703.06757v1.
- [46] M. Abramowitz and I. A. Stegun, *Handbook of Mathematical Functions with Formulas, Graphs, and Mathematical Tables* (Dover, New York, 1964).